Department of Biomedical Sciences
University of Veterinary Medicine Vienna

Institute of Physiology, Pathophysiology and Biophysics

Unit of Physiology, Pathophysiology and Experimental Endocrinology

Head: Erben, Reinhold; Univ.-Prof. Dr. med. Dr. med. vet.

The effect of FGF23 on inflammation and collagen regulation in various models of ischemic heart disease

Diploma Thesis

University of Veterinary Medicine Vienna

Submitted by

Flora Klinger

Vienna, 2021

Supervisor

Univ.-Prof. Dr. med. Dr. med. vet Reinhold Erben,

Head of the Institute of Physiology, Pathophysiology and Biophysics,

Unit of Physiology, Pathophysiology and experimental Endocrinology of the University of Veterinary Medicine of Vienna

Veterinärplatz 1,

1210 Vienna

Declaration of honor

“I declare on my word of honour that I have written this paper on my own and that I have not used any sources or resources other than stated and that I have marked those passages and/or ideas that were either verbally or textually extracted from sources. This also applies to drawings, sketches, graphic representations as well as to sources from the internet.

The paper has not been submitted in this or similar form for assessment at any other domestic or foreign post-secondary educational institution and has not been published elsewhere.
The present paper complies with the version submitted electronically.”

Date: 31.03.2021 Signature

Acknowledgements

I would like to express my gratitude to all those who supported me during my study and in the preparation of this thesis.

First of all, I would like to thank my former colleague Kristopher Ford, without whom this work could not have been possible. I would like to thank you for your willingness to provide information and expertise, the provision of several documents and last but not least your patience. Thank you for showing me what is possible.

Moreover I would like to thank my Mentor Mrs. Ass.-Prof Dr. rer. nat. Priv.-Doz. Olena Andrukhova. Thank you for your encouraging, understanding, and motivating manner. You always inspired us with your passion and your dedication and tried to involve us in your team in every way possible. You are deeply missed, and your experience will continue within our daily work.

Furthermore, I would like to thank Prof. Dr. med Dr. med. vet Reinhold Erben, for taking over the supervision of my thesis under these circumstances. Without your support I would not have been able finishing my studies and following my passion as veterinarian focusing on small animals. Thank you for your encouragement and never-ending patience.

Thank you to Petra Heidler and Gerald Forstner who supported me in the revision of this thesis and for sharing your experience with me.

Additionally, I would like to thank Clemens Salner. Thank you for supporting me in everything I do and understanding my priorities in stressful times. You are the best.

A special thank also to my brother Nicolaus Klinger and his wife Jazmin Sol Terroso, who spent many evenings supporting me as a matter of course.

Finally, I would like to thank my parents Richard Klinger and Renate Klinger-Sturzlbaum, who made this study possible through financial but also mental support. Thank you for always believing in me, for showing me my strengths when I couldn't see them and for making it possible to pursue my dream job.

Flora Klinger,

Vienna, March 2021

Abstract in english

Fibroblast growth factor 23 (FGF 23) is a bone secreted hormone, which belongs to a group of signal mediators and plays important roles in many physiological mechanisms. It acts mostly via binding to a receptor complex consisting of FGF receptors (FGFR) and the co-receptor α-Klotho. Due to the fact that FGF 23 also appears to be involved in some pathological processes, it has increasingly become subject of research.

In this study, I have focused on FGF 23 and its role in inflammation, more specifically in the cardiac inflammatory response and collagen deposition in ischemic heart tissue. Therefore cardiomyocytes isolated from hearts of mice that underwent an myocardial infarction surgery were used, as well as isolated fibroblasts to see if FGF 23 has an impact on collagen turnover. I hypothesized that FGF 23 is a regulator of inflammation and collagen deposition during these pathological conditions. My aim is first to investigate whether an increase in FGF 23 concentrations stimulates per se an inflammatory pathway or if it results from a Pro-inflammatory impulse, and second to clarify how collagen turnover take place in myofibroblasts after myocardial infarction. In this experiment I used tree-months old male wild-type (WT) mice, as a control group, as well as FV-, KV- and VDR knockout mice, which were housed under 12 hours light/dark cycles at a temperature of 24 degrees and were fed with rescue diet. In order to answer the research questions, the concentrations of inflammatory markers (IL-10, Il-6), collagen activators (MMP9, ADAM 10) and collagen type 1 and type 3 were compared in different heart tissue (ischemic versus non-ischemic), as well as in vehicle treated and recombined FGF treated cardiac fibroblasts. To analyse the results, a multifactorial, a single-factorial ANOVA and t-tests were carried out and results with a p-value of 0,05% were considered significant.

The results suggest that FGF 23 increases fibroblast proliferation, which has a vast impact in remodelling after myocardial infarction in the ischemic tissue. In summary, it can be said that, FGF 23 increases a pro-inflammatory response and regulates collagen in the absence of a pro-inflammatory stimulus and secondly, after the activation of a proinflammatory pathway, specifically a myocardial infarction in this context, FGF 23 seems to stimulate collagen type 1 activity.

This study shows an coherent overview of the molecular changes in various tissue models after myocardial infarction and is intended to provide an incentive for further research.

Abstract in german

Fibroblast growth factor 23 (FGF23) ist ein Hormon aus der Gruppe der Signalmediatoren, welches aus Knochen sezerniert wird und in vielen physiologischen Abläufen eine wichtige Rolle spielt. Seine Wirkung entfaltet es hauptsächlich über einen Rezeptor-Komplex, bestehend aus FGF Rezeptoren und dem Co-Rezeptor α-Klotho. Aufgrund der Tatsache, dass FGF 23 neben sein physiologischen Effekten auch in einer Reihe von pathologischen Prozessen beteiligt zu seien scheint, ist es in den letzten Jahren immer mehr in den Fokus der Forschung gerückt.

Da FGF 23 unter pathologischen Bedingungen im Herzen produziert wird, wurde der Schwerpunkt dieser Arbeit auf die Rolle von FGF 23 in der Entzündungsreaktion am Herzen, sowie der von FGF 23 verursachten Ablagerung an Kollagen im kardialen Gewebe unter ischämischen Umständen, gelegt. Um ischämische Bedingungen zu simulieren, wurden Kardiomyozyten aus Herzen von genetisch variierenden Mäusen (Kontrollgruppe, FGF 23-, Klotho- bzw VDR- Defizienz) isoliert, welche zuvor einer Operation unterzogen wurden, in der experimentell ein Myokard Infarkt ausgelöst wurde. Somit konnte die Auswirkung einer genetischen FGF 23 und Klotho-Defizienz auf pro-inflammatorische Gene und die Kollagenproduktion im Herzen unter pathologischen Bedingungen untersucht werden. Weiters wurde isolierte Fibroblasten herangezogen, um die Auswirkung von FGF 23 auf den Kollagenumsatz zu veranschaulichen, da diese verantwortlich für die Kollagenproduktion sind.

Das Ziel dieser Arbeit ist es, einerseits herauszufinden ob die Steigerung an FGF 23 Serum Konzentrationen ursächlich für eine Entzündungsreaktion im Herzen ist oder ob diese durch einen pro-inflammatorischen Stimulus hervorgeht. Andererseits sollte untersucht werden, wodurch es, nach einem Myokard Infarkt, zu vermehrter Kollagen Produktion in Myofibroblasten kommt.

In diesem Experiment wurden drei Monate alte wild-type (WT) Mäuse als Kontrollgruppe herangezogen, sowie FV-, KV-, und VDR-knockout Mäuse, welche unter 12 Stunden Tag/Nacht Zyklen bei einer Käfigtemperatur von 24 Grad gehalten wurden und mit einer Spezialdiät gefüttert wurden.

Um die Forschungsfragen zu beantworten, wurden die Konzentrationen von Entzündungsmediatoren (IL-10, IL-6), Kollagen Aktivatoren (MMP9, ADAM 10) und von Kollagen Typ 1 und Typ 3, in ischämischen und nicht-ischämischen Herzgewebe, sowie in

den unterschiedlich behandelten Fibroblasten (vehicle behandelte Zellen als Kontrollgruppe und mit rekombinanten FGF23 behandelt Fibroblasten), verglichen.

Um die Resultate auszuwerten wurde eine multifakorielle und eine einzelfaktorielle ANOVA und ein t-test durchgeführt. Resultate ab einem p-Wert von 0,05% wurden als signifikant gewertet.

Auf Grund der Resultate der in-vitro-Daten mit kultivierten kardialen Fibroblasten lässt sich vermuten, dass FGF 23 die Kollagen Typ 1 Produktion und manche pro-inflammatorische Gene stimuliert und somit einen bedeutenden Einfluss auf den Umbau der extrazellulären Matrix zu haben scheint.

Zusammenfassend kann angenommen werden, dass FGF 23 eine Entzündungsreaktion fördert und unter Voraussetzung eines Myokardinfarktes, die Kollagen Typ 1 Aktivität stimuliert.

Diese Studie soll einen Überblick über die molekularen Veränderungen in verschiedenen Gewebemodellen nach einen Myokard Infarkt aufzeigen und somit einen Anreiz auf weiterführende Studien bieten.

Contents

Abbreviation

AMI	Acute myocardial infarction
Ang I & II	Angiotensin I and II
ATP	Adenosintriphosphat
BCP	1-bromo-3-chloropropane
CKD	Chronic kidney disease
DLD	Diagnosen und Leistungsdokumentation der österr. Krankenanstalten
DMEM	Dulbecco's Modified Eagle's Medium
ECCM	Extracellular collagen matrix
ESRD	End-stage real disease
ET-1	Endothelin 1
FBS	Fetal Bovine Serum
FGF	Fibroblast growth factor
FGF 23	Fibroblast growth factor 23
FGFR	Fibroblast growth factor receptor
FGFR4	Fibroblast growth factor receptor 4
ICR	Intercostal region
IL-1	Interleukin 1
IL-6	Interleukin 6
IZ	Infarct zone
LCA	Left coronary artery
LDCA	Left descending coronary artery
LVH	Left ventricular hypertrophy
MI	Myocardial infarction

MMPs	Matrix metalloproteinases
NIZ	Non-infarct zone
P4H	prolyl-4-hydroxylase
PTH	Parathyroid hormone
RAAS	Renin-angiotensin-aldosterone system
RCA	Right coronary artery
rFGF	Fibroblast growth factor 23 receptor
TGF-$_{1}$	Transforming growth factor $_{1}$
TNF-	Tumor necrosis factor
WT	Wild type

1 Introduction

In recent years, fibroblast growth factors (FGF), which are a group of signal mediators consisting of 22 members, have increasingly become subject of research due to the fact that they are involved in a wide variety of physiological and pathological processes. The FGF cellular actions range from proliferation, survival, cell migration and differentiation to more negative effects such as fibrosis, inflammation and cell death, depending on the target tissue (FAUL et al., 2011).

From a closer look on the role of FGFs in the heart, previous studies showed that these signal mediators could induce cardiac remodeling under physiological conditions as well as exert pathologic effects. Even though cardiac myocytes are differentiated cells, it is necessary that they are able to respond to local and circulating FGFs in situations of increased demand. These situations can range from pregnancy or physical work-out, with physiologic hypertrophy as well as the need to promote angiogenesis to increase cardiac function and output (FAUL, 2016). Nevertheless, this FGF mediated scenario might also become a pathological situation where elevated serum FGF concentrations aggravate the underlying disease (FAUL, 2016). For example, it is known that increased fibroblast growth factor 23 (FGF 23) directly targets cardiac myocytes and leads to cardiac hypertrophy in chronic kidney disease (CKD) patients. This condition is called uremic cardiomyopathy (FAUL, 2016).

1.1 Background of the study

Heart diseases, particularly coronary artery disease, contribute to a large part to the mortality rate in the human population and, since possibilities for cure are very limited, there is a need for new therapeutic approaches. The FGF 23 has been recognized as an important factor in the etiology of heart disease and therefore has increasingly come into focus of research. Important findings showed that FGF 23 serum concentrations in CKD patients are up to 1000 times higher than in healthy individuals and that FGF 23 can directly induce left ventricular hypertrophy (LVH) (FAUL et al., 2011). Initially, the question was whether FGF 23 was a mediator or a biomarker for the severity of CKD and whether a statement about the prognosis could be made using FGF 23 serum level determination. As the physiological role of FGF 23 is to maintain phosphate homeostasis by increasing renal phosphate excretion, the connection between increased FGF 23 in CKD patients might be explained by the loss of kidney function and therefore a reduced renal capacity for phosphate excretion. This leads to

hyperphosphatemia and to an increased FGF 23 synthesis in bones. Other studies suggest that inflammation and disorders in the iron homeostasis are responsible for increasing FGF 23 levels in early CKD (DAVID et al., 2016). With the important knowledge that FGF 23 can directly induce LVH, independent of kidney function, fundamentally new questions have arisen. What causes cardiac hypertrophy and what part of the pathway is FGF 23 dependent? Traditionally it was believed that cardiovascular events in CKD happen due to hypertension but the findings in individuals with normal kidney function gives the perspective of new explanations. Some studies have shown that FGF 23 is potentially able to induce an inflammatory response and displays immunomodulatory and pro-fibrotic properties (DAVID et al., 2016). With the prior knowledge that ischemic heart disease is very widespread in the human population, there is an urgent need to create new therapeutic approaches. Moreover, the knowledge that FGF 23 seems to have a direct influence on changes in the shape of the heart, indicates the need for further research. The assumption can be made, that FGF 23 is a regulator of inflammation and fibrosis after myocardial infarction. Also, we can assume that LVH may arise secondary to ECCM remodeling, resulting in the aim of this study, which is to investigate if FGF 23 is involved in the cardiac inflammatory response and collagen deposition in ischemic heart disease.

1.2 Research objectives

Due to the fact that FGF 23 induces LVH in healthy individuals, who do not suffer from a history of CKD, new approaches need to be considered: it should not be assumed that LVH develops secondary to hypertension, but that FGF 23 leads directly to LVH via unknown control loops. As many members of the FGF family are able to induce fibrosis and even former studies suggested that FGF 23 is significantly involved in the fibrosis of heart tissue (HUIXIN et al., 2016), the central hypothesis of this study is that FGF 23 is a regulator of inflammation and collagen deposition in ischemic heart disease. The development of LVH in CKD patients can certainly be explained by increased pressure load on the heart, due to hypertension, which causes the heart to beat against increased resistance. Since the kidneys contribute decisively to regulating blood pressure, hypertension is a common finding when kidney function declines. Nevertheless, previous studies state that FGF 23 directly induces LVH (FAUL et al., 2011), regardless of kidney function. Therefore, it can be suggested that FGF 23 leads to collagen deposition and that the resulting decrease in elasticity of the tissue may be responsible for the alterations of the heart.

In pursuit of the findings from previous studies, the aim of this work is to understand pathological processes in ischemic heart disease patients and to establish possible control loops for remodeling cardiac tissue, following coronary insufficiency. Therefore, I hypothesize that FGF 23 is a central regulator in cardiac tissue transformation after an acute myocardial infarction (AMI) and plays an important part in collagen deposition leading to fibrosis.

In the current thesis, two different questions should be answered: on one hand, taking into account that molecular changes occur in the entire heart after MI, what role does FGF 23 plays under these conditions? And on the other hand, what impact does FGF 23 have on the cellular changes in the ECCM, after prolonged ischemia? To test the hypothesis that FGF 23 regulates inflammation and collagen deposition in heart tissue, the situation of the right ventricle and septum, where physiological conditions should prevail was compared to the left ventricle, where ischemia was induced by an acute myocardial infarction surgery in three month old mice. In addition, a control group of mice was selected that had the same conditions of a surgery, but in which no ligation of the left descending coronary artery (LDCA) was performed and therefore no clinical MI was triggered. In these scenarios the investigations focused on the pro-inflammatory cytokine IL-1, Grp18, which is a receptor inducing a proinflammatory response, collagen regulators, ADAM and MMP9, as well as the expression of collagen I and III. In addition, the situation in fibroblasts was of interest, as these cells are known to convert into myofibroblasts and to produce collagen. The effect of recombinant FGF 23 in these cells is of particular interest but the stimulus of a combination of a proinflammatory cytokine and recombinant FGF 23 in fibroblasts was also considered. Thus, the aim of these investigations was to provide further insights into the molecular changes in the heart tissue after an AMI.

2 History and introduction into the topic

In general, cardiovascular diseases are the most common cause of adult death worldwide, in approximately 30% of the cases. The statistics show a clear upward trend considering the past decades due to the fact that many heart diseases are influenced by exogenous behavioral risk factor, such as tobacco consumption, diet and physical inactivity. While infectious diseases and malnutrition dominated before 1900, cardiovascular diseases became the most serious medical condition in the 20th and 21st century due to lifestyle changes and improved medical care (GAZIANO and GAZIANO, 2012).

Heart failure is a clinical syndrome, caused by inherited or acquired abnormality of cardiac function or structure, which occurs in many different conditions including valvular heart disease, cardiomyopathy, myocarditis, neoplasia, trauma, pericardial or vascular disease as well as ischemic heart disease. Typical symptoms range from dyspnea and fatigue to other signs such as edema or rales. Among numerous etiologies of heart failure, for example chronic pressure or volume overload, I focus on coronary artery disease, potentially leading to myocardial infarction and its impact on the cardiac tissue (MANN and CHAKINALO, 2012). The adult mammalian heart lacks sufficient regenerative potential to replace cardiac muscle cells once an injury caused necrosis, leading to major therapeutic problems. Although various drugs and devices can temporarily improve cardiac function and are therefore necessary to increase life expectancy, once cardiac cells are lost, they cannot be replaced in a lifetime (XIN et al., 2013). New therapeutic approaches for heart regeneration and repair, for example stimulation of dedifferentiation and proliferation of cardiomyocytes are currently subject of research (XIN et al., 2013).

2.1 Histological structure of the heart

The four-chambered heart is a hollow muscular organ with characteristic wall layering and it contains different cell types. The outermost layer- the epicardium- has a serous membrane and in its fatty layer there are coronary vessels embedded that are responsible for the blood supply to the heart. The middle layer underneath, the true muscular wall of the heart is called myocardium and it consists of four different cell types: atrial and ventricular cardiomyocytes, fibroblasts, endothelial and smooth muscle cells. The cardiomyocytes are terminally differentiated and they develop tension by shortening, whereas Pacemaker cells and Purkinje fibers are specialized cardiomyocytes, which are able to generate and conduct electrical

impulses. Therefore, these special cells are responsible for the heart's ability to beat. The fibroblasts are flattened elongated cells giving structural support and passing electrical signals. These very important dynamic cells respond to mechanical and chemical stimuli and play an active role in producing and maintaining extracellular matrix. The endothelial and smooth muscle cells are vessel components, building the capillary microcirculation that serves the contractile unit assembly. The innermost layer, known as the endocardium, is made out of endothelial cells and it builds the interior lining of the heart (BAUM and DUFFY, 2011; XIN et al, 2013). In a healthy heart, the myocytes, which contributes with mechanical and electrical properties, build less than half of the cell population. Studies have shown, that 90 to 95% of the non-myocyte cell mass consist of fibroblasts, showing the importance of these structural cells. Moreover, they are able to produce most of the matrix macromolecules with collagen type I and III, which are the main representatives of structural proteins (BODH, 2003).

2.2 Ischemic heart disease

Ischemic heart disease is a condition in which there is a mismatch between oxygen demand and supply to a portion of the myocardium, most commonly caused by inadequate blood flow of a coronary artery. The task of these vessels, with an average diameter of 1-3,5 mm in humans, is the oxygen and energy supply to the muscular layer of the heart and therefore they are essential for the functionality of the organ. A lack of perfusion of the myocardium leads to myocardial ischemia and consequently, to the cell death of cardiomyocytes. The main cause of the illness is arteriosclerosis, which leads to deposits in the vessels (arteriosclerotic plaques), causing the stiffening of the walls and the loss of elasticity in arteries. This results in a decreasing vessel diameter and, thus, in coronary insufficiency. The coronary sclerosis usually arises from endothelial damage from endogenous and exogenous toxins. In order to understand the pathogenesis, it is necessary to take a closer look at wall and cell structure of blood vessels. The outermost layer is the Tunica adventitia which contains the vasa vasorum. The middle layer is made up of smooth muscle cells, collagen and elastic fibers and it is called Tunica media. In this context, the Tunica interna, which represents the innermost layer, is of special interest (ALBES and BUTTER, 2019). It consists of two different cell types: fibrophilic and atherophilic cells. Atherophilic cells have a strong tendency to absorb and accumulate lipids and are therefore able to form atheriosclerotic plaques, which contain blood components, cholesterol and mycopolysaccharides, showing that exogenous factors such as diets high in cholesterol or fat can influence the incidence rate. This type of coronary artery narrowing leads

to ischemia and subsequently myocardial infarction (NETTER, 2000). Although, arteriosclerosis is seen most frequently in ischemic heart disease patients, there are other causes of coronary insufficiency, for example thrombosis, embolism, vasculitis, coronary spasm or compression of the coronary arteries from the outside due to neoplastic tissue or heart hypertrophy. Also an increase in oxygen demand, as occurs in cardiac hypertrophy, certain forms of cardiomyopathy, valvular heart disease, hyperthyroidism, hypertension, infectious diseases and fever can result in similar symptomatologies. The most common cause of death in the industrialized nations is ischemic heart disease with chronic course. Although, the numbers have been declining since 1970, statistics from Statistic Austria show that cardiovascular disease, with 38.9 percent and a total number of 32 684 people, was the second most common cause of death in Austria in 2018 (STATISITK AUSTRIA, 2019). According to the „Diagnosen- und Leistungsdokumentation der sterreichischen Krankenanstalten“ (DLD), approximately 20 000 people were diagnosed with an acute myocardial infarction in 2011. Men had a 2,5 percent higher incidence rate than women and older people a higher than younger. For the years 2002 to 2011, there is no clear development in the myocardial infarction (MI) incidence rate; although since 2007, there has been a slight downward trend with an average 2,6 percent per year (BMSGPK, 2019). Therefore, myocardial infarction still plays a significant role in the human population. The risk factors include genetic predisposition, age, gender - men are more at risk than women-, hypercholesterolemia, arterial hypertension -with critical values of a systolic blood pressure higher than 125 mmHg and a diastolic higher than 85 mmHg-, smoking and diabetes mellitus (Bundesärztekammer, 2019).

2.3 Physiology of the different heart models

2.3.1 Ischemia

Ischemia describes a pathological condition in which restricted or impaired blood flow causes a lack of oxygen supply to tissues or organs. It is one of the main three sources of hypoxia in tissues, along with arterial hypoxemia, described as a reduced oxygen partial pressure in arterial blood, and anemia, a condition of reduced oxygen capacity due to a lack of erythrocytes. Ischemia can occur in many organs at the same time, as it is the case of a circulatory shock, in which the blood circulation is centralized and only supplies the vital organs, or localized in one organ due to vascular occlusion (GROS, 2010). The heart itself is able to utilize many different substrates such as glucose, free fatty acids, lactic acid or ketone

bodies, thus it is thus well protected against lack of energy. The situation is different with oxygen: the high content of mitochondria in myocardium cells illustrate the capacity to use oxygen and the high level of dependence on an adequate oxygen supply. Under anaerobic conditions the heart, in contrast to skeletal muscle, can only provide very little energy and fatigue occurs very quickly. Therefore hypoxia and not a reduction in energetically usable substrates, is a primary cause of disease symptoms in case of circulatory disorders (HARMEYER and TOBIAS, 2010). There is a difference between absolute ischemia, in which complete cessation of blood flow is characteristic, and relative ischemia, in which blood flow is insufficient. Atherosclerosis is a common example of the narrowing of blood vessels in the sense of a stenosis. Any type of circulatory disturbance leads to hypoxia in the affected tissue, thus, to an impairment of the cellular metabolic processes and can consequently cause functional loss. Persistent ischemia leads to necrosis of muscle cells located in the supply area of the affected coronary artery.

2.3.2 Ischemia – Reperfusion

Reperfusion damage is the clinical picture that is triggered by the restored blood circulation after prolonged hypoperfusion, which can affect limbs or organs. Reperfusion paradox is intended to describe the contradiction that re-perfusion can lead to additional harm. The pathology is based on an oxygen deficiency, which leads to a complete degradation of adenosine triphosphate (ATP) within a few minutes. ATP is considered a universal supplier of energy to the cell and a lack of it leads immediately to an increase of hypoxanthin. In addition, due to the loss of function of ATP-dependent ion pumps, there is a potassium outflow from the cell and calcium influx into the cell. These conditions lead to a conversion of the enzyme Xanthindehydrogenase into Xanthinoxidase, which is able to oxidize hypoxanthin in xanthin, in the presence of oxygen, as is the case with reperfusion. Free oxygen radicals, such as superoxide, hydrogen peroxide and hydroxyl radicals are able to cause cell membrane damage by lipid peroxidation. As a result, the damage of the previous ischemia is multiplied. Further destruction is due to the fact that cell damage by free oxygen radicals can increase the expression of adhesion molecules, so-called selectins, stimulating neutrophilic granulocytes to enhanced binding to the vascular endothelium. As a consequence, white blood cells increasingly migrate into the surrounding tissue, in order to release free oxygen radicals and other messenger substances, such as platelet activating factor and leukotrienes. In turn, these signaling molecules attract more neutrophilic granulocytes that accumulate in

the damaged tissue. The resulting vicious circle aggravates the event immensely by the constant formation of harmful oxygen radicals and stimulation of white blood cells. The resulting tissue damage leads to a massive increase in the permeability of the endothelial membrane and thus to a further formation of local edema (GROS, 2010; MARIAN, 2007).

2.3.3 Myocardial infarction

Myocardial Infarction describes the irreversible cell death of cardiomyocytes, caused by local circulatory disorders in a limited area of the heart muscle. The causal reason for this pathology is an acute or prolonged occlusion of a coronary artery, which is almost always stenosed beforehand. The ischemia tolerance of the myocardium is about two to four hours, within which reperfusion can lead to a complete restoration of function. After this period of time, necrosis and irreversible damage of cardiac muscle cells in the affected supply area occurs, leading to inflammatory reaction and loss of function (NETTER, 2000). The extent of myocardial damage depends on different factors such as the territory of the affected vessel, the duration of occlusion, the quantity of blood supplied by collateral vessels and the demand for oxygen of the myocardium (ANTMAN and LOSCALZO, 2012). Myocardial Infarction can be classified according to their location and extent. One possibility is to divide into antero-, posteroseptal or lateral regions, describing the localization of the affected area. Another possibility is to differentiate into transmural or non-transmural damage, expressing whether necrosis affects all layers of the heart or only subendocardial areas (NETTER, 2000). The different areas of the heart muscle can be affected, depending on which vessel is abnormally changed and which section of the heart muscle is supplied with blood by the respective vessel. The general rule is: the closer the occlusion is to the aorta -the more proximal to the vessel-, the larger the infarct area; the further away, the smaller the less perfused area. Statistically, more patients are affected by occlusion of the left coronary artery (LCA) than of the right coronary artery (RCA). This can be explained by the larger area of the left ventricle, and thus, a larger number of blood vessels, that supply the blood requirement. Common symptoms include sudden, persistent, often severe chest pain, which predominantly radiates to the left shoulder, arm, back and upper abdomen, fear of death, nausea, vomiting and dyspnea. In the acute phase, dangerous cardiac arrhythmias and ventricular fibrillation, followed by sudden cardiac death, can be life-threatening. Unlike humans, where non-infectious causes are predominantly reported, this type of myocardial infarction is rarely seen in animals. Although a similar pathogenesis may occur in some animal species that reach old age, such as parrots and other

zoo animals (Pacific walrus), infectious causes outweigh non-infectious causes of myocardial infarction in domestic mammals (GRUBER et al., 2002). Often, in these individuals endocarditis of the mitral valve leads to the detachment of thrombi into the coronary arteries and, thus, to the obstruction of these small vessels. In addition, domestic dogs in rare cases develop amyloidosis of small arteries of the heart, causing reduced oxygen supply to the heart muscle, but these usually remain clinically unrecognized and are only detected in pathological examinations as local scarring of the heart muscle (DRIEHUYS et al., 1998).

2.4 Pathological remodeling after myocardial infarction

The capacity of the heart to remodel after a pathological event such as myocardial infarction, cardiomyopathy, hypertension or valvular heart disease is a complex and dynamic process that allows to adjust ventricular size and shape; it is therefore necessary to maintain adequate cardiac output after cardiomyocyte necrosis. The scenario is divided into an early phase, which occurs within 72 hours of injury and it is defined by infarct expansion resulting from degradation of inter-myocyte collagen struts in the infarct zone and a late phase, which involves the ventricle globally, characterized by progressive dilatation, distortion of ventricle shape and mural hypertrophy due to extracellular matrix degradation in the non-infarct zone. The goal of these alterations is the formation of a scar, to stabilize the contractile function and to distribute the increased wall stresses more evenly. After a myocardial infarction, injured and necrotic myocytes release pro-inflammatory cytokines, for example Transforming growth factor β_1 (TGF-β_1), which initiate migration of macrophages, monocytes and neutrophils into the infarct zone and localizes inflammatory response. TGF-β_1 is also responsible for fibroblast chemotaxis and proliferation and differentiation of fibroblasts to myofibroblasts. Myofibroblasts are able to synthesis collagen type I and III due to the fact that they express genes encoding for procollagen and receptors for angiotensin (Ang) II, TGF-β_1 and endothelin-1 (ET-1), which stimulates the autoregulation of collagen turnover, a complex process modulated by several factors that is not fully understood yet. Collagen deposition happens to be found mainly in the infarct zone, that leads to the formation of a scar and therefore structural support with simultaneous loss of function. Current observations show an early increase in collagen type III starting on day two after a pathological event and a later but longer elevated concentration of collagen type I mRNA incipient on day 4 after myocardial infarction. After 28 days, the necrotic myocytes are entirely replaced by fibrous tissue and after the formation of a scar, collagen

formation is down-regulated and most myofibroblasts undergo apoptosis (BODH, 2003; SUTTON and SHARPE, 2000).

2.5 Introduction of inflammation and collagen

Collagen represents a heterogeneous group of proteins and it is one of the most important fiber constituents in different tissues in human and animal bodies. There are many known different types of collagen that provide tensile strength to the tissue in physiological conditions. Although collagen is an important component of almost any tissue, an excess or a deficit of it can lead to loss of function. On one hand, an excessive accumulation of collagen is often detrimental but on the other hand, collagen degradation and loss after myocardial infarction is associated with infarct expansion and subsequent functional decline (RICH et al., 2005). The construction of collagen molecules is complex: in its ultrastructure, it forms a superhelix, consisting of 3 α chains, which wind around each other. The most important fibrillar components of the cardiac extracellular matrix are collagen type I and type III, which are produced by myofibroblasts and represent the main structural protein in tissues. The two types differ significantly in their microscopic appearance and their structural role in the extracellular matrix: Collagen type I is associated with predominantly thick fibers that confer tensile strength and resistance to stretch and deformation, while collagen type III corresponds to thin fibers that confer resilience. As mentioned above, the collagen biosynthesis occurs in myofibroblasts, involving several enzymatic steps and it is influenced by many different factors, such as prolyl-4-hydroxylase (P4H), different growth factors, like transforming growth factor β_1 (TGF-β_1), insulin growth factor and connective tissue growth factor, cytocines such as tumor necrosis factor-α (TNF-α) and interleukin-1 (IL-1) and various hormones and enzymes. Under physiological conditions the extracellular collagen matrix (ECCM) consists of 85% collagen type I, 11% collagen type II and 4% of other matrix components (BODH, 2003). This distribution changes after myocardial infarction, as a regional remodeling of the ECCM takes place, contributing significantly to the global heart structure. In order to get an overview of the processes and to understand how structural changes appear, it is necessary to briefly go into more detail on the pathogenesis. Myocardial infarction, as a result of arteriosclerotic alterations, causes, due to oxygen deficiency, cellular damage to myocytes, non-myocytes and the ECCM in the infarct zone leading to vascular changes in the whole heart. At molecular levels, modifications take place in both areas, the infarct zone (IZ), where orderly degradation of the ECCM, mediated by matrix metalloproteinases (MMPs) with following reparative fibrosis

occurs but also an increase of interstitial collagen in the non-infarct zone (NIZ). At a macroscopic level it can be seen that this kind of ventricular dysfunction, due to cell damage leads to volume overload and subsequent progressive dilation as well as reactive hypertrophy of the heart. However, remodeling of the extracellular collagen matrix plays a major role in ventricular remodeling after myocardial infarction, whereby a very small decrease in collagen below normal, a disruption and/or a defective composition can lead to drastic consequences, such as left ventricular dilation and rupture. Contrarily to this a 2- to 3-fold increase in myocardial collagen above the normal level results in an increased stiffness but only a mild dysfunction (BODH, 2003).

2.6 Effects of fibroblast growth factor 23

Fibroblast growth factor 23 (FGF 23) is a circulating hormone, which is secreted mainly by osteocytes, osteoblasts and venous sinoids in the bone, but it is also expressed in endocrine organs, such as the parathyroid gland, ovaries and testes, the heart and parts of the central nervous system. Its most important physiological role is to maintain phosphate homeostasis by increasing renal phosphate excretion in situations of hyperphosphatemia. To achieve this, it intervenes in the downregulation of activity and expression of the sodium-dependent phosphate transporters NaPi-2a and NaPi-2c in the proximal tubule of the kidney. The main task is to limit intestinal phosphate absorption and to inhibit renal phosphate reabsorption (David et al, 2016). Other physiological effects range from reducing renal synthesis, stimulating the degradation of 1,25-dihydroxy-vitamin D ($1,25(OH)_2D_3$) and the stimulation of the distal tubular sodium and calcium reabsorption. In summary, it can be said that FGF 23 is a bone secreted hormone, which influences mineral metabolism in the kidney as its main target organ. FGF23 acts mostly via binding to a receptor complex consisting of FGF receptors (FGFR) and the co-receptor α-Klotho but a Klotho-independent signaling, for example in cardiac tissue, has also been described. The FGF 23 production in the bone is predominantly regulated by phosphate load and $1,25(OH)_2D_3$ but there is evidence that additional factors such as calcium intake, parathyroid hormone (PTH), the renin-angiotensin-aldosterone system (RAAS), oxidative stress and parameters of the iron metabolism can influence the FGF 23 synthesis. In addition to the very important physiological actions of FGF 23, there has been increasing interest in the pathological effects of elevated serum FGF 23 concentrations in recent years. FGF 23 excess due to a primary hereditary over-production causes hypophosphatemia and inadequately low $1,25(OH)_2D_3$ levels, leading to clinical consequences of rickets, osteomalacia

and bone deformities. Increased FGF 23 concentrations often show extrarenal effects including inhibition of PTH secretion in the hyperplastic parathyroid gland, impairment of host defense due to its interactions with the immune system, alterations of the neuronal morphology and synaptic density leading to cognitive dysfunction and induction of myocyte hypertrophy resulting in left ventricular hypertrophy. To get into more detail about the pathological effects of elevated FGF 23 levels, I would like to take a closer look at the situation in chronic kidney disease patients, where its concentrations rise progressively with a declining kidney function. This phenomenon can be explained due to the fact that the loss of kidney function is associated with a declining capacity of the kidney to excrete phosphate, leading to hyperphosphatemia which triggers FGF 23 secretion in bones with the goal to keep serum phosphate concentrations within normal limits. Thus, the remarkable effects of the disease are illustrated with CKD patients showing 1000-fold higher FGF 23 concentrations than healthy individuals. Additionally, left ventricular hypertrophy is frequently observed in end-stage renal disease patients (ESRD), which is traditionally explained by risk factors, such as hypertension and volume overload. This explanation seems to be obvious, since the healthy kidney is significantly involved in the regulation of blood pressure. In recent clinical studies, elevated FGF 23 serum concentrations are shown to be associated with the presence of enhanced left ventricular mass index and risk of LVH, independent of kidney function, in various clinical settings, which offers a new perspective and leads to the conclusion that FGF23 directly induces left ventricular hypertrophy. Moreover, it was also identified that fibroblast growth factor receptor 4 (FGFR4) is mediating the cardiac effects of FGF23 as the FGF 23-stimulated cardiac hypertrophy in vitro was completely blocked in the presence of an FGFR4 inhibitor. As Klotho is not expressed in cardiac myocytes, it is thought that FGF23 acts directly in a Klotho-independent manner on cardiac myocytes to cause cardiac injury. As LVH in CKD patients is strongly associated with cardiovascular disease events and death, several studies have manipulated FGF23 with the aim to determine whether it is a mediator or just a biomarker of increased mortality risk (DAVID et al., 2016; HAFFNER and LEIFHEIT-NESTLER, 2016).

Other interesting observations have been made regarding the interaction of FGF 23 with the immune system and its role in inflammation. Commonly, CKD patients suffer from chronic inflammation and it has been found that FGF 23 levels are significantly associated with pro-inflammatory cytokines, for example interleukin-6 and oxidative stress markers. Additionally pro-inflammatory macrophages express FGF 23, which enhances tumor-necrosis factor-. This findings reinforces the suspicion that FGF 23 acts as a pro-inflammatory cytokine regulating

$1,25(OH)_2D_3$ synthesis in macrophages and may modulate immune responses. Further studies (ROSSAINT et al., 2016) have also shown that FGF 23 is believed to inhibit neutrophil activation and migration by deactivating neutrophil integrin, which is necessary for endothelial adhesion and consequently for leukodiapedesis. This leads to the assumption that FGF 23 is a negative regulator of host defense (HAFFNER and LEIFHEIT-NESTLER, 2016). Finally, it should be mentioned that significant associations between elevated FGF 23 serum levels, arterial stiffness and vascular calcification that leads to atherosclerosis have been reported. Nonetheless, more precise mechanisms are still subject of research (HAFFNER and LEIFHEIT-NESTLER, 2016).

3 Methods

3.1 Overview

For the purpose of this work, it is important to differentiate two topics: the first relates to the entire heart and it is intended to provide insights into the initial molecular reaction of the organ after acute myocardial infarction. The second relates to the molecular changes at cellular levels, induced by FGF 23 and addresses the question whether FGF 23 is able to influence ECCM remodeling.

Animal models and genetic background

First, in this study were used three-month-old male mice of different genotypes, bred by intercrossing heterozygous animals on a C57BL/6 genetic background including wild-type mice (WT), animals that do not express the gene encoding for FGF 23 (FV), as well as mice that lack the co-receptor of FGF 23 (KV) and vitamin D receptor (VDR) animals (ERBEN et al., 2002). All mice were housed under 12 hours light/dark cycles at 24 with ad libitum access to water and a rescue diet containing 2,0 % calcium, 1,25 % phosphorus, 20 % lactose and 600 IU vitamin D/kg (Ssniff, Soest, Germany) or a normal diet containing 1,0 % calcium, 0,7 % phosphorus and 1000 IU vitamin D/kg (Ssniff). As it is necessary in every investigation, WT mice were incorporated as a control group but due to the fact that previous studies have shown that a vitamin D deficiency can potentially increase the incidence of myocardial infarction, homozygous vitamin D receptor mutant mice with functionally inactive VDR on rescue diet were also of interest for this study. Although, other studies (FORD et al., 2018) discovered that the VDR mice appear to show similar results as the WT control group, once they were fed with a so-called rescue diet, this genetic group was included in order to exclude or confirm vitamin D deficiency as the cause of molecular changes. The purpose of feeding VDR animals with rescue diet is to prevent secondary hyperparathyroidism, which occurs due to the loss of VDR function in the small intestine, leading to a calcium absorption defect and therefore hypocalcaemia in VDR mice on normal diet. It has been suggested by former studies (FORD et al., 2018), that the secondary hyperthyroidism rather that the lack of vitamin D is responsible for the negative impact on cardiac function after myocardial infarction. Under physiological conditions vitamin D receptors are found in cardiomyocytes, endothelial cells and macrophages in the heart (FORD et al., 2018). Moreover, FV animals do not express the gene encoding for FGF 23, which is particularly important in this context. Lastly, KV mice were

included because they lack Klotho -the co-receptor for FGF 23- on a genetic basis and therefore they are of interest to answer the question if FGF 23 acts Klotho dependently or independently in certain scenarios. Each individual genotype group was further divided into two subgroups: A sham group in which animals underwent surgery, to provide same conditions potentially caused by anaesthesia or tissue trauma, but the decisive intervention to trigger MI was left out and the MI group whose animals were subjected to myocardial infarction surgery. This results in a total of eight different groups for the first major question. To look deeper into the experiments, each heart of every group was divided into the left ventricle, in which the tissue has experienced hypoxemia from a myocardial infarction and into the right ventricle and septum, where no ischemia should have occurred.

Secondly, at the cellular level, isolated fibroblasts were of interest, as these structural cells are known to produce collagen. To answer the second major question, fibroblasts were left untreated, as a control, represented in the “Veh” group, treated with recombinant FGF 23, a proinflammatory cytokine (IL-1) or a combination of recombinant FGF 23 and IL-1.

3.2 Research design and method

3.2.1 Acute myocardial infarction surgical model

For this experiment we used tree-months old male WT mice, which were housed under 12 hours light/dark cycles at 24 with ad libitum provisions of tap water and rescue diet. The rescue diet (Ssniff, Soest, Germany) contained 2,0 % calcium, 1,25 % phosphorus, 20 % lactose and 600 IU vitamin D/kg.

In this model, acute myocardial infarction was induced by permanent ligation of the left descending coronary artery (LDCA). Mice were anaesthetised by intra-peritoneal injection using ketamine (100 mg/kg intra-peritoneal, Narcetan©, Vetoquinol GmbH, Ismaning, Germany) and medetomidine (0,25 mg/kg intra-peritoneal, Narcostart©, Richter Pharma AG, Wels, Austria) and placed under controlled ventilation with room air. Next, left lateral thoracotomy was performed at the 4^{th} intercostal region (ICR) and the pericardium was removed to provide access to the left descending coronary artery. The ligation was placed one to two mm below the tip of the left atrial appendage using a 7–0 prolene suture. Then the pericardium was repositioned and the chest and the skin re-sutured. In order to control infection and to ensure a good pain management, mice were treated with antibiotics (Enrofloxacin 10 mg/kg every 24 hours, Baytril©, Bayer Vital GmbH, Leverkusen, Germany)

and buprenorphine (0,05 mg/kg, Bupaq©, Richter Pharma AG, Wels, Austria) and their weight was monitored daily for the first five days, to detect possible health deterioration as early as possible. If one of the animals showed a poor state of health, it was euthanized according to a humane endpoint. The sham operation was performed as above with absence of coronary artery ligation. The mice were weighed weekly with daily check-ups until necropsy at two weeks after surgery (FORD et al., 2018).

3.2.2 Molecular biology

Homogenization

The first step in the RNA isolation protocol is homogenization of tissue samples in TRI Reagent solution. TRI Reagent solution is a complete reagent for the isolation of total RNA, DNA and protein from diverse biological material. It combines phenol and guanidine thiocyanate in a monophasic solution to rapidly inhibit RNase activity. Therefore, tissue or cultured cells were homogenized in 1 ml TRI Reagent solution per 5-10 x 10^6 cells or per 10 cm^2 culture dish area. Then, the homogenate was incubated for five minutes at room temperature and, as a final step, it was centrifuged at 12000 x g for 10 minutes at 4 . The centrifugation removes insoluble material from homogenates that contain high amounts of protein, fat, polysaccharide or extracellular material, such as muscle. Subsequently, the supernatant was transferred to a fresh tube (Applied Biosystems, 2010).

RNA extraction

To prepare the samples for RNA extraction, we homogenized them as described above. During the next step, we added 100 µl 1–bromo–3–chloropropane (BCP) per 1 ml TRI reagent solution and it was incubated at room temperature for eight minutes. This was necessary to separate the homogenized solution into an aqueous and an organic phase and the incubation time allowed nucleoprotein complexes to completely dissociate. It was then centrifuged at 12000 x g for 15 minutes at 4 . As the RNA partitions to the aqueous phase, the desired phase was transferred to a fresh tube. The organic phase, consisting of proteins, was discarded. Next, 500 µl of 100 % isopropanol was added per 1 ml of TRI reagent solution to precipitate RNA from the aqueous phase and it was vortexed for ten seconds. Afterwards the solution was incubated at -20 for 30 minutes. As an additional step, the mixture was centrifuged at 12000 x g for eight minutes at 4 . The supernatant was removed carefully without disturbing the pellet and was discarded afterwards. Precipitated RNA formed a gel-like or white pellet on

the side and bottom of the tube. Finally, the RNA was washed with 1 ml of 75 % ethanol per 1 ml of TRI reagent solution, centrifuged at 12000 x g for eight minutes and then the ethanol was removed. To prepare 75 % ethanol we mixed 250 μl nuclease-free water with 750 μl 100 % ethanol per ml of TRI Reagent solution. This step was repeated two times and then the RNA pellet was air dried for 8 minutes. For solubilization we dissolved the RNA in 20–30 μl RNAse free water, depending on the pellet size, by vigorous vortexing. For RNA analysis we used the NanoDrop 1000 A spectrophotometer, which determines the concentration of a RNA solution by measuring its absorbance at 260 nm. For sample quality control, we used the A_{260}/A_{280} ratio of the RNA as an indication of its purity. The total RNA should have an A_{260}/A_{280} ratio of 1,8 – 2,2. RNA yield is dependent on factors such as sample type, thoroughness of the sample disruption and sample handling (modified Protocol from: Applied Biosystems, 2010).

Reverse transcription

The goal of the reverse transcription protocol is to produce complementary DNA (cDNA). Samples were prepared in a laminar flow chamber in a molecular biology laboratory, while using UV light. For that, RNA samples were mixed with a calculated amount of RNAse free water and 10 μl of an Master Mix. The Master Mix contained Reverse Transcriptase Buffer, 25 dNTPs, Reverse Transcriptase Primers, RNAse Inhibitor, nuclease free water and reverse transcriptase enzyme (50 U/ml). Every component was kept frozen until the very end and we worked on ice during the entire process. The samples were vortexed to ensure that all products at the bottom of the Eppendorf tubes were well mixed and the cDNA program was used on the Cycler AB 1 PCR machine.

Real-time PCR

The real-time PCR, also called quantitative PCR or qPCR, is a simple method to determine the amount of a target sequence or gene that is present in a sample (Applied Biosystems, 2011). In contrast to normal PCR, in which it is detected whether a specific gene is present or not, after a predetermined number of amplification cycles, the produced amount of DNA in qPCR is analysed after each cycle. One of the mentioned amplification cycle includes: “melting”, -a process where hydrogen bonds are broken at 94–96 and that is necessary to separate the double-stranded DNA-; “primer annealing“ at around 55–65 -where primers of a certain nucleotide sequence can attach and, “elongation” as a final step, in which a DNA-

polymerase, starting at the 3'-end of the primer, doubles the DNA sequence of interest. As a result, data are related in terms of numbers, allowing easy analysis of fold change in an experiment. This method relies on control genes to normalize data from sample to sample. Therefore, at least control genes should be chosen that do not change during treatment. There are different methods to detect quantitative real-time amplification: for example, the DNA binding dyes, which is considered as a non-specific method and the hydrolysis probes, considered as a specific procedure. Nonetheless, it is important to differentiate these two methods. First, the DNA binding dyes, is the earliest method developed for real-time PCR. It involves the use of for example Ethidiumbromid or SYBR Green© being common representatives and binding to the minor groove of double-stranded DNA. The change, in fluorescence in the sample, is monitored by a fibre optic cable and a spectrofluorometer. This is possible due to the accumulation of double-stranded PCR products and that the signal increases together with the amount of DNA increases. Secondly, hydrolysis probes are labelled with fluorescent substances at the 5'-end and a quencher at the 3'-end. When the two reporters are in proximity, the fluorescent signal is quenched. During the annealing step, the probe gets degraded and the fluorophore is released from the effects of the quencher, which results in an increasing fluorescence. The major advantage in this method is time: qRT-PCR can yield an answer in just a few hours by only requiring nanogram quantities of RNA. Also, qRT-PCR uses fluorescent reporters, which is an enormous advantage in comparison to northern blots, using mostly radioactive probes. Nonetheless, there is the disadvantage of the need of special equipment: qRT-PCR does require a special thermal cycler with fluorescent detection capabilities, as qRT-PCR uses fluorescent reporters. In summary, qRT-PCR answers questions about the presence of a gene of interest, and whether the level of the transcript has changed under an experimental condition (Promega RNA Analysis Notebook).

In order to answer the scientific questions different genes of interest were chosen, referred to a housekeeping gene (OAZ) and the quantity was determined by real-time PCR.

Gpr18 is a receptor, which activation contributes to the resolution of a proinflammatory response as it is known to be elevated in proinflammatory stimulated macrophages (M1 macrophages) but not in anti-inflammatory stimulated macrophages (M2 macrophages) (TAKENOUCHI et al., 2012).

IL-1 is known to be a proinflammatory cytokine and it is counted among inflammation mediators. It is elevated during early healing phases and are able to activate MMPs (BODH, 2003).

Matrix metallopeptidase 9 (MMP9): is an enzyme, which is known for several important functions, such as degradation of extracellular matrix, activation of IL-1and also myocardial remodeling. Among its substrates are collagen type 1 and type 3 and therefore it promotors collagen breakdown (BODH, 2003).

A Disintegrin and metalloproteinase domain-containing protein 10 (ADAM10) is a protein and has a broad specificity for peptide hydrolysis reactions (AMOUR et al., 2000), which make both of them, MMP9 and ADAM 10, collagen regulators.

Collagen 1A1 and **Collagen 3A1** are components of the extracellular matrix and their ratio is decisive in how elastic or stiff the tissue appears. Collagen fibrils are responsible for structural support, tensile strength (collagen type 1) and resilience (collagen type 3) (BODH, 2003).

While **IL-6** is one of the interleukins that regulate inflammatory response in the organism, **IL-10** has an inhibitory effect on defence reactions and thus, protects the body against excessive inflammation.

Alpha- smooth muscle actin) is a protein of smooth muscle cells and plays an important role in fibrogenesis, as its activation has a key role in development of the fibrotic response (CHERNG et al., 2008).

3.2.3 Primary cell isolation

Fibroblast solation protocol

During the first step in our fibroblast isolation protocol, hearts were removed from the mice's thorax and placed into an ADS buffer, while the dish was kept on ice. The ADS buffer contained 6,8 g NaCl, 4,76 g HEPES, 0,12 g NaH_2PO_4, 1 g Glucose, 0,4 g KCl and 0,1 g $MgSO_4$ per liter. It was adjusted to pH 7.35, filtered and stored at 4 . After dissection, each heart was checked individually for exact preparation, blood clots on the surface and in the atrium were removed, and the hearts were transferred into a new ADS buffer, just enough to cover the hearts, while placing the new dish on ice. It was important to work swiftly, as hearts should not be kept at low temperatures for too long. During the next step the tissue of the hearts were cut until it was homogenised using "spring bow" scissors. In order to have a size specification, the tip of a Pasteur pipette was used as a reference: tissue pieces should have been small enough to pass through it. Then, the heart pieces were drawn up together with the ADS buffer and transferred into a Duran bottle. Next, the buffer was carefully drawn up and discarded with a

sterile Pasteur pipette by tipping the bottle and rotating it to separate heart pieces from the buffer. Thus, the preparatory steps were done and the actual enzyme digestion could be started. To this end, an enzyme mix was prepared, consisting of 0,03 g collagenase type 2 (Worthington Biochemical Corporation cat no LS0004176 (310 U/mg DW), kept at 4) and 0,03 g pancreatin from porcine pancreas (Sigma P3292-25G, kept at -20). The enzymes were weighed into two separate 50 ml Falcon tubes, 20 ml ADS buffer was added and each falcon was vortexed to dissolve. Then, the enzymes were filtered sterilized using syringe filters of 0.2 μm and the filtered enzymes were added to a sterile 100 ml Duran bottle. Additionally, the Falcon tubes were washed with another 10 ml ADS buffer, resulting in about 50 ml of enzyme solution. The heart pieces were digested in six steps using an adjusted protocol, described as follows: For the first digestion step, 10 ml of enzyme mixture was added to the bottle with minced hearts and placed into a shaking water bath at 180 strokes per minute for 5 minutes. After the incubation time, they were removed from the water bath and the supernatant was discarded. In the second digestion step, 10 ml of enzyme solution was added and the heart tissue was digested at 160 strokes per minute for 20 minutes. The enzyme volume for the third and fourth step was 8 ml with an incubation time of 25 minutes and a speed of 150 strokes per minute. In the fifth round 6 ml enzyme mixture was used with an incubation time of 15 minutes and a speed of 160 strokes per minute. Finally, 6 ml enzyme solution was used again and the tissue was placed into the shaking water bath for 25 minutes with 150 strokes per minute. After each digestion, except the first, the supernatant was transferred to a sterile falcon tube containing 2 ml Fetal Bovine Serum (FBS), centrifuged for 5 minutes at 1000 rpm, the supernatant was removed and the falcons were placed in the incubator. Next, the pellet was tapped to loosen it, 4 ml FBS was added and re-suspended. For every digestion (step two to five) the procedure was repeated using one tube to spin and the other to incubate cells. After the final step, the supernatant was transferred to the tube containing all the cells and centrifuged it at 1000 rpm for 6 minutes. Then, the supernatant was then carefully pipetted off and the pellet was re-suspended in plating media, consisting of 340 ml Dulbecco's Modified Eagle's Medium (DMEM, Lonza, Basel, Switzerland), 85 ml Medium 199 (M199), 50 ml horse serum, 25 ml fetal calf serum and 5 ml of a Penicillin-Streptomycin (*100) solution in 500 ml. As a standard, 4 ml plating media were used on five hearts and were adjusted accordingly when needed (Adult Fibroblast Isolation Protocol from Kristopher Ford).

Culture and treatment of the cells

First, as a pre-plating step, one 60 mm uncoated primary dish was used per five hearts, 4 ml of the suspension was added to each dish and it was placed on a tray in the incubator for at least one hour, to remove adherent non-myocytes. Then, the pre-plates were washed with plating medium using a Pasteur pipette to remove the medium containing myocytes from plate one and transferred it to a 50 ml tube. Afterwards, 4 ml fresh plating medium was added to the plate. Moreover, the medium was removed from plate two as before in a 50 ml tube, the medium was transferred from plate one to plate two and another 4 ml fresh plating medium was added to plate one. The washing was repeated, as with plates one and two, and the media was moved to a 50 ml tube until each plate had been washed three times. It was necessary to wash thoroughly to remove as many myocytes as possible but it was important not to touch the surface on the plate with the tip of the pipette. Then, the Falcon tube contained all the myocytes that should be counted and plated out. In order to plating out the cells, 180 μl of Trypan Blue (Gibco, cat no 15250-061) and 20 μl cell suspension was added to a sterile 1,5 ml Eppendorf tube and mixed well. Then, it was then applied to a haemocytometer, five squares were counted out and the volume of cell solution necessary per plate to reach a number of 3,5 x 10^6 for a 60 mm dish was calculated. The cells were plated out on a 1 % gelatine coated primary dish and incubated overnight in the incubator at 37 and 5 % CO_2 concentration.

Establishment of a primary cardiomyocyte isolation protocol using modified Langendorff set-up

The invention of retrograde mammalian heart perfusion, by Oscar Langendorff in 1895, has proven invaluable in the development of our current understanding of heart physiology and it has remained at the forefront of scientific research. It is still one of the main tools for analyzing the mechanisms of myocardial physiology and cellular signaling. The advantages of this preparation include simplicity, low cost, reproducibility, the ability to study the organ in isolation of other organ systems and its wide species applicability (BELL et al., 2011). According to Langendorff's original description, the hearts were perfused by cannulating the aorta, which led to a retrograde flow, and Tyrodes Solution was used as a buffer. Moreover, with the perfusion buffer flowing opposite to normal physiologic flow, the aortic valve was closed under pressure. In the original description, the preparation was perfused under constant pressure, but in our set-up, the mode of constant flow perfusion was chosen (Adapted Protocol from

Kristopher Ford) (GRAHAM et, al., 2013; LOUCH et al., 2001). For the Tyrodes Solution, a glass container was filled with five liters of double distilled water and placed on a heat plate stirrer. Then a magnetic stirrer was added and the temperature was set to 37 Next, 33.89 mg of sodium chloride (NaCl), 8.4 mg of sodium hydrogen carbonate ($NaHCO_{3)}$,0.2839 mg of di-sodium hydrogen orthophosphate (Na_2HPO_4), 1.232 mg of magnesium sulphate–7–hydrate ($MgSO_4$-$7H_2O$) and 1.864 mg of potassium chloride (KCl) was added. Once all ingredients were fully dissolved, one liter was separated and 1.8 ml calcium chloride ($CaCl_2$) and 1.98 g glucose was added in the same manner as described above, using accurately measured amounts. It was important to only add the metabolic substrates on the day of the experiment. For the modified Langendorff perfusion protocol, three months old C57BL/6 mice were used, which were euthanized by cervical dislocation. Hearts were removed and coronary arteries perfused via the aorta at a constant pressure of 73.5 mm Hg (37) with Tyrodes solution gassed with 95 % oxygen and 5 % CO_2 at pH 7.4. In order to isolate cardiomyocytes, the heart was first perfused with Tyrodes + Ca + glucose, then with Tyrodes + glucose for three minutes each. After that, a glucose, collagenase I and protease-enriched Tyrodes solution was used for a four-minute perfusion. To prepare the enzyme solution, 245 U/ml of collagenase type 2 and 0.9 U/ml protease type XIV into 50 ml Tyrodes + glucose were mixed. This solution was re-used during the 4-minute perfusion. As a next step the solution was exchanged with Tyrodes + glucose + BSA to perfuse the heart for further five minutes. To prepare this solution, 4,6 mg/ml bovine serum albumin was added to a Tyrodes solution. Then, the hearts were removed from the canula, the atria were excised and the remaining heart tissue was cut into small pieces. Finally, five Falcon tubes were used with 5 ml Tyrodes+Glucose+BSA and the tissue was agitated for two minutes each time. Then, the tissue was examined macroscopically and the detached cells in the supernatant microscopically.

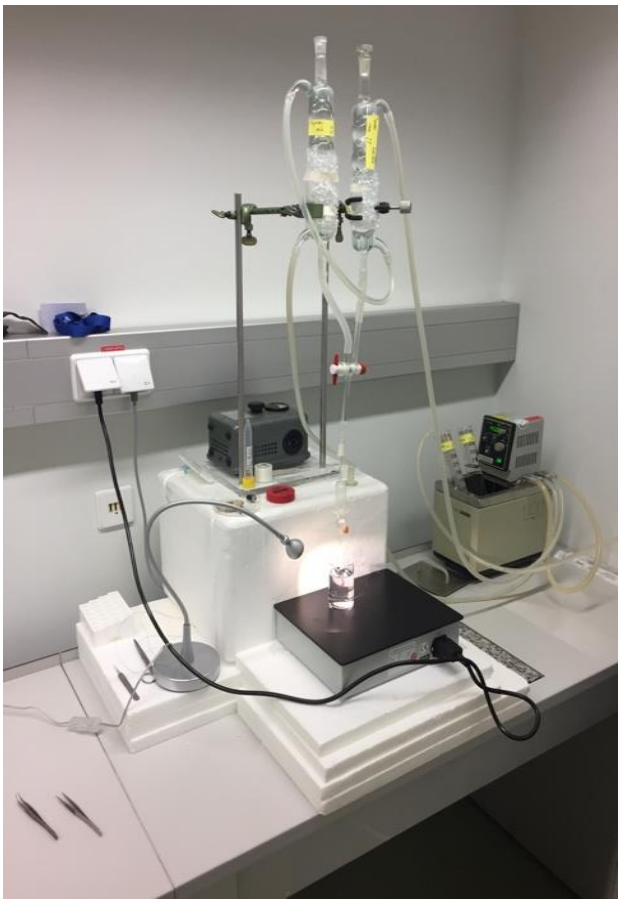

Figure 1: *Photography of the exact Langendorff set-up used in the experiment. The heart is placed in a glas container filled up with Tyrodes solution (A), sitting on a heating plate (B) set to 41℃ to provide a fluid temperature of 37℃. The two glas falcons (C) are filled up with Tyrodes solution gassed with 95% oxygen and 5% CO_2 at pH 7.4, one of them additionally provided with glucose and BSA. The desired solution for the perfusion can be changed using the rotary valve*

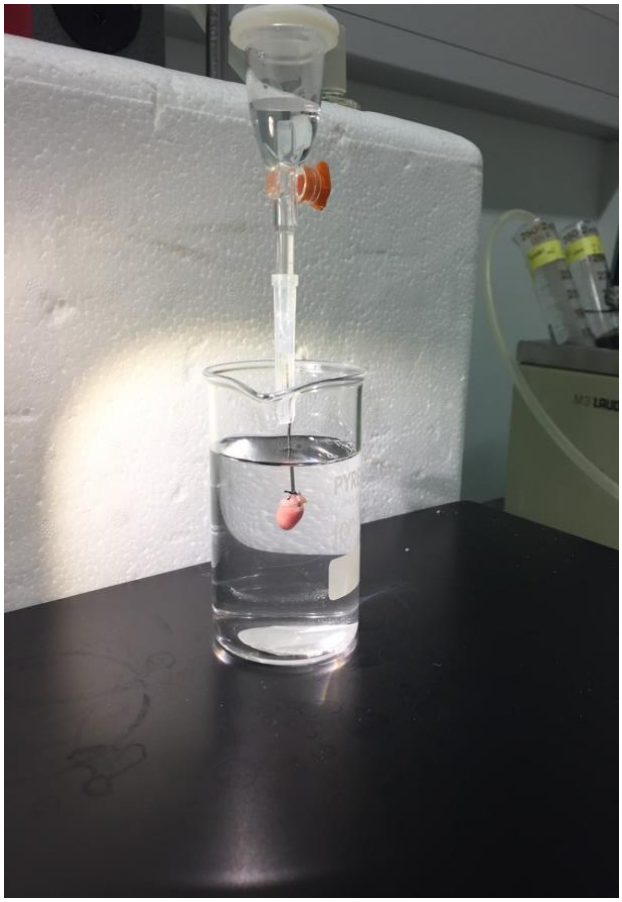

Figure 2: *close up Photography of an isolated heart of a mice placed on a cannula to perfuse. Therefore a freshly prepared heart was positioned on a conventional cannula and fixated on the aorta using any surgical suture. The heart was placed in and perfused with Tyrodes solution gassed with 95% oxigen and 5% CO_2 at pH 7.4*

3.3 Statistical methods

The following methods were used to analyze the results:

A multifactorial ANOVA analysis was used to compare the effect of specific genes on the two different mice groups (sham and MI) for each genotype. This analysis was done for the right ventricle and septum (figure 3) and the left ventricle (figure 4). Furthermore a Levene-Test was performed in order to test for homogeneity of the variances. In case of homogeneity of variance, the Games Howell method was chosen and in case of inhomogeneity of variance the LSD method was chosen for post-hoc-analysis.

To analyze the isolated fibroblasts, which underwent different treatments (untreated, IL-1ß and IL-1ß+fFGF23), a t-test was carried out per gene of interest (figure 5). To test for homogeneity of variance a Levene-F-test was performed.

A one-factor ANOVA was carried out to check the differences in the treatment of the isolated fibroblasts according to Veh, IL-1ß and IL-1ß+rFGF 23 for each examined gene (figure 6). Again a Levene test was used to check for homogeneity of variance and the corresponding post-hoc method (LSD or Games Howell) was applied.

The SPSS software was used for statistical analysis and results with a p-value of 0,05% was considered significant.

3.4 Hypothesis formulation

1. Scientific question: Does FGF 23 trigger an inflammatory response after a myocardial infarction?
   Hypothesis: FGF 23 causes a proinflammatory stimulus after myocardial infarction.

2. Scientific question: Does FGF 23 stimulate remodeling of the extracellular matrix (ECCM) in heart tissue?
   Hypothesis: FGF23 stimulates fibroblasts to produce collagen after an inflammation.

4 Results

As already mentioned above, this chapter is divided into two different parts to answer the research questions. In order to answer the first research question, figure 3 provides an overview of the molecular events in the right ventricle and septum, representing non-ischemic tissue, and figure 4 visualizes the situation in the left ventricle, where ischemia occurred. At the beginning of each figure an overview of the graphs is shown in order to get an impression of the molecular events in each tissue type (ischemic vs. non-ischemic), followed by a detailed description and the data analysis of each gene of interest.

Additionally, in order to answer the second research question, a focus was placed on fibroblasts, as these cells are known to produce collagen and are involved in ECCM remodeling. For this purpose, vehicle treated cells were used as a control group, as well as cells treated with recombinant FGF 23 (figure 5), IL-1ß or a combination of IL-1ß and recombinant FGF 23 (figure 6).

In the analysis, the following variables were defined and the tested mice were divided into the following groups:

genotype (WT, VDR, KV, FV)

infarction status (MI, Sham)

treatment status (Veh, rFGF 23, IL-1ß, IL-1ß+rFGF 23)

4.1 Myocardial infarction experiments

Overview figure 3: right ventricle and septum

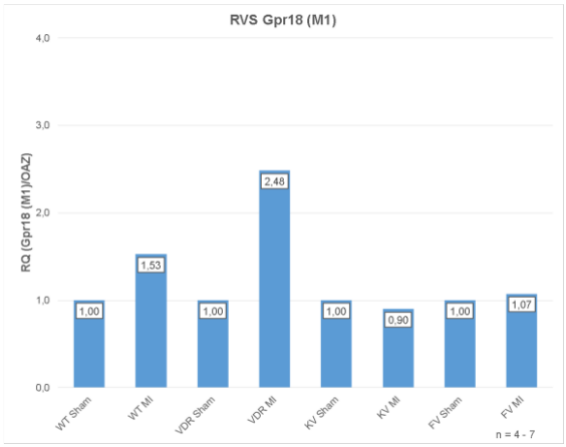

figure 3A

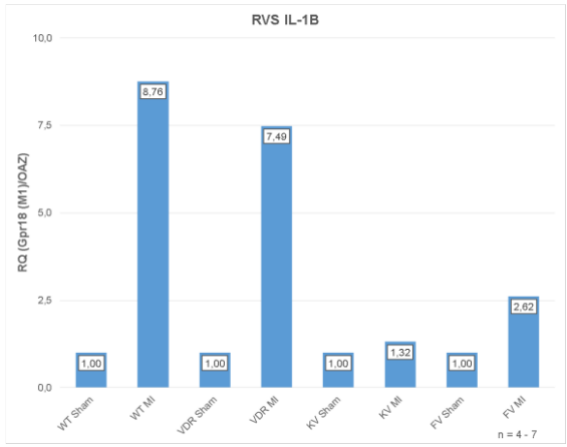

figure 3B

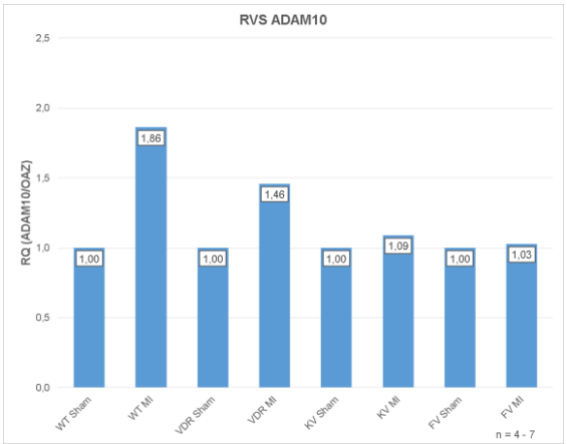

figure 3C

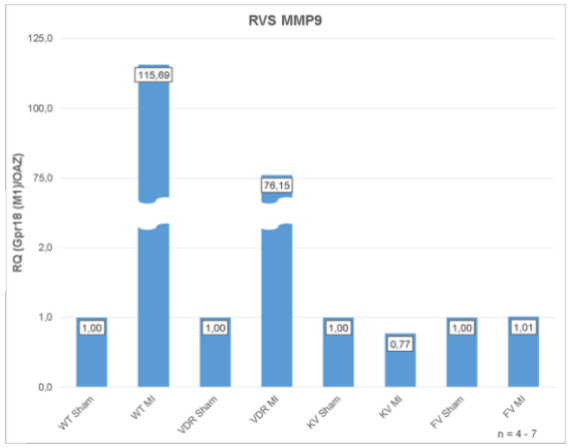

figure 3D

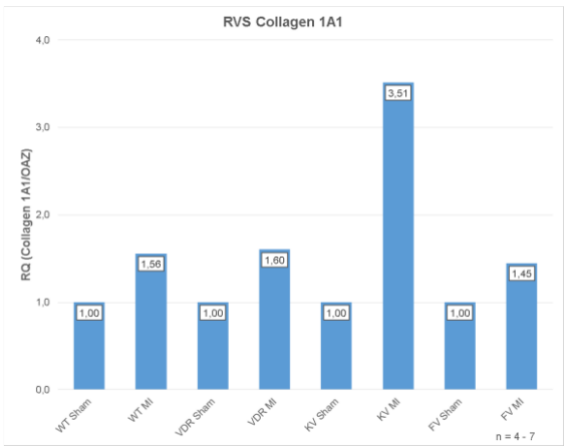

figure 3E

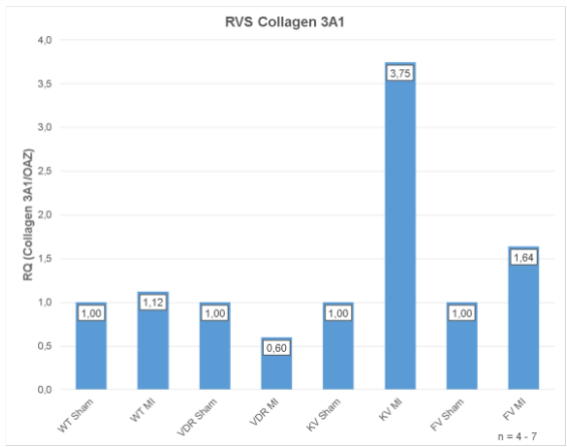

figure 3F

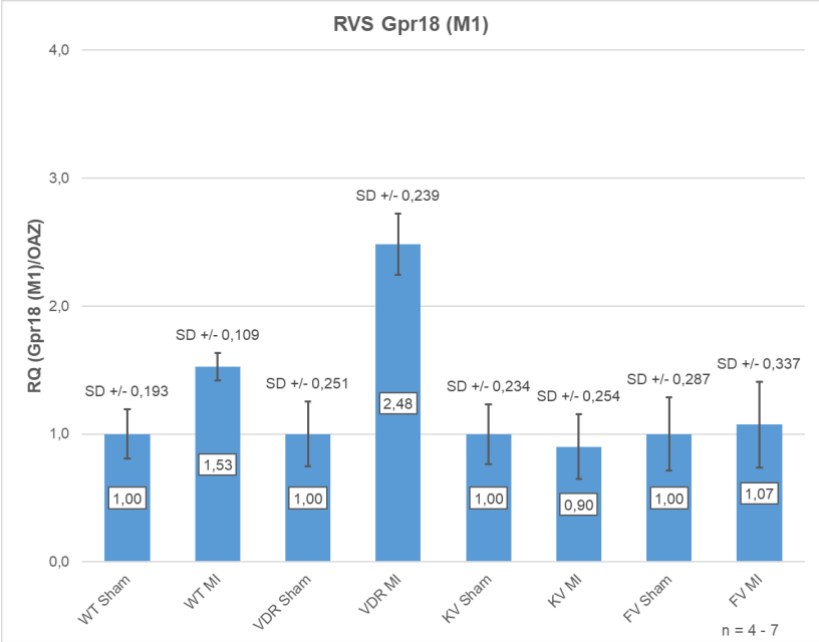

Figure 3A: RQ Gpr18-OAZ according to infarction-status and genotype

Source	F - value	p - value	partial eta Squared
Corrected Model	2.298	0.047	0.297
Intercept	6,242.238	0.000	0.994
infarction-status * genotype	2.436	0.080	0.161
infarction-status	5.77	0.021	0.132
genotype	1.426	0.250	0.101
Adjusted R Squared	0.168		

table 1A: 2-way ANOVA, gene of interest Gpr18

Figure 3A shows the RQ values of Grp18 in the right ventricle and septum for all groups. The results of the multifactorial ANOVA analysis for Grp18 are shown in table 1A. Hereby it can be seen that the overall statistical model is significant (p=0,047) which means that the variables (genotype and infarction-status) do have an effect on RQ. Looking at each of the variables independently reveals a statistically significant effect on RQ (F=5,77; p=0,021) for the variable infarction-status and a non-significant effect for the variable genotype (F=1,426; p=0,250). This means that the tested mice show a significantly different RQ value for Gpr18 depending on the infarction-status.

Furthermore, it can be shown that the effect of infarction-status on RQ does not depend on the genotype because both variables interact non-significantly (F=2,436; p=0,080).

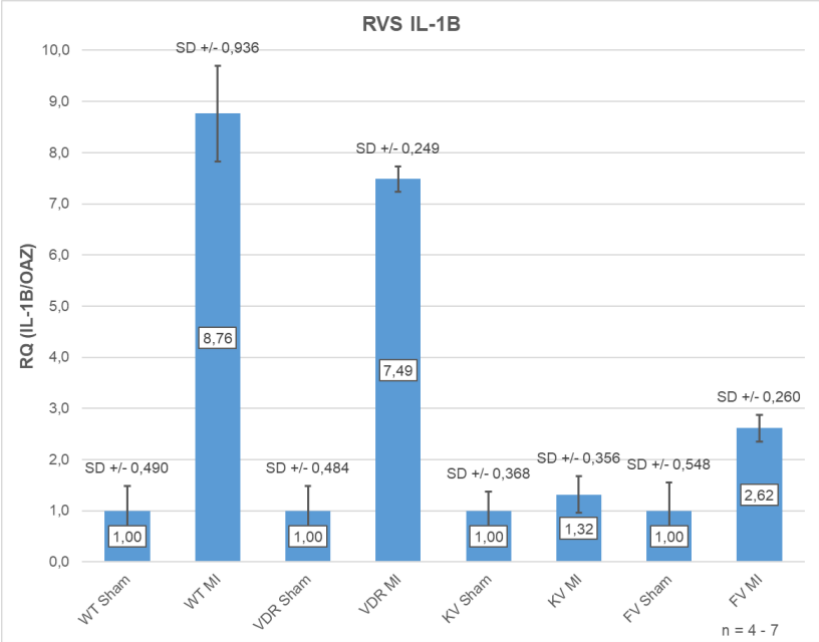

figure 3B: RQ IL-1ß-OAZ according to infarction-status and genotype

Source	F - value	p - value	partial eta Squared
Corrected Model	6.489	0.000	0.558
Intercept	1,406.532	0.000	0.975
infarction-status * genotype	2.905	0.048	0.195
infarction-status	27.867	0.000	0.436
genotype	4.883	0.006	0.289
Adjusted R Squared	0.472		

table1B: 2-way ANOVA, gene of interest IL-1ß

Figure 3B shows the RQ values of IL-1ß in the right ventricle and septum for all groups. The results of the multifactorial ANOVA analysis for IL-1ß are shown in table 1B. Hereby it can be seen that the overall statistical model is significant (p=0,000) which means that the variables (genotype and infarction-status) do have an effect on RQ. Looking at each of the variables independently reveals a statistically significant effect on RQ (F=27,867; p=0,000) for the variable infarction-status, as well as a significant effect for the variable genotype (F=4,883; p=0,006). This means that the tested mice show a significantly different RQ value for IL-1ß depending on the infarction-status and genotype.

Furthermore, it can be shown that the effect of infarction-status on RQ depends on the genotype because both variables interact significantly (F=2,905; p=0,048).

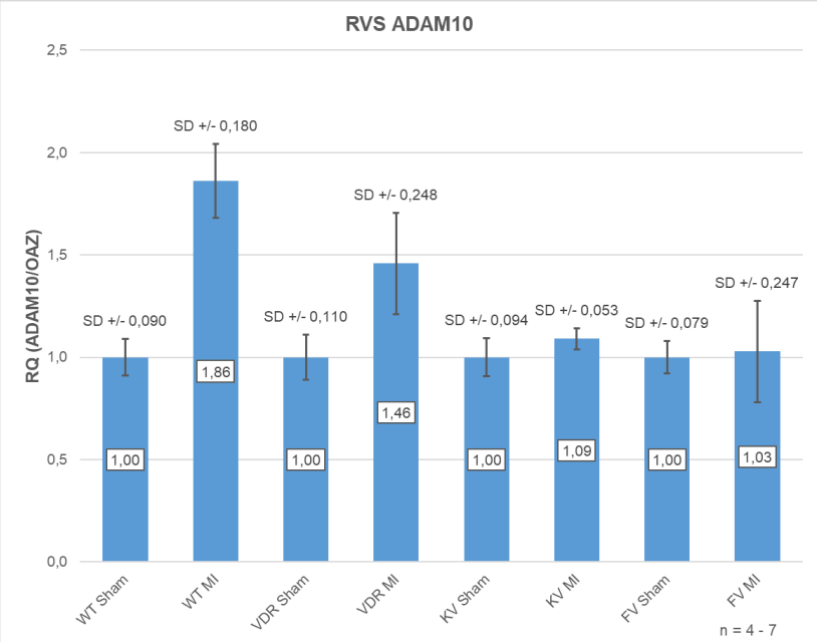

figure 3C: RQ ADAM10-OAZ according to infarction-status and genotype

Source	F - value	p - value	partial eta Squared
Corrected Model	5.407	0.000	0.513
Intercept	852.585	0.000	0.959
infarction-status * genotype	4.460	0.009	0.271
infarction-status	17.525	0.000	0.327
genotype	2.457	0.079	0.170
Adjusted R Squared	0.418		

table1C: 2-way ANOVA, gene of interest ADAM10

Figure 3C shows the RQ values of ADAM10 in the right ventricle and septum for all groups. The results of the multifactorial ANOVA analysis for ADAM10 are shown in table 1. Hereby it can be seen that the overall statistical model is significant (p=0,000) which means that the variables (genotype and infarction-status) do have an effect on RQ. Looking at each of the variables independently reveals a statistically significant effect on RQ (F=17,525, p=0,000) for the variable infarction-status and a non-significant effect for the variable genotype (F=2,457, p=0,079). This means that the tested mice show a significantly different RQ value for ADAMS10 depending on the infarction-status.

Furthermore, it can be shown that the effect of infarction-status on RQ depends on the genotype because both variables interact significantly (F=4,46, p=0,009).

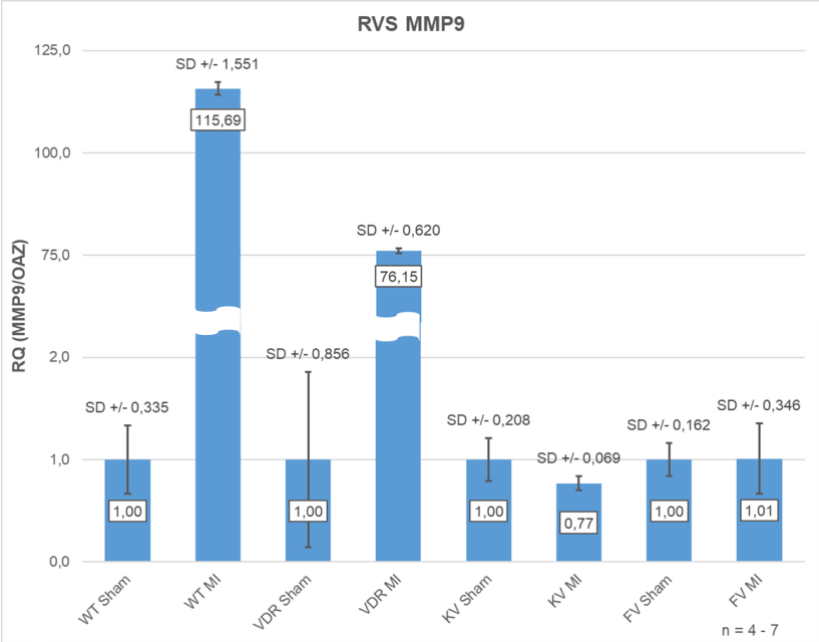

figure 3D: RQ MMP9-OAZ according to infarction-status and genotype

Source	F - value	p - value	partial eta Squared
Corrected Model	16.499	0.000	0.752
Intercept	414.739	0.000	0.916
infarction-status * genotype	14.404	0.000	0.532
infarction-status	38.086	0.000	0.501
genotype	17.473	0.000	0.580
Adjusted R Squared	0.707		

table1D: 2-way ANOVA, gene of interest MMP9

Figure 3D shows the RQ values of MMP9 in the right ventricle and septum for all groups. The results of the multifactorial ANOVA analysis for MMP9 are shown in table 1D. Hereby it can be seen that the overall statistical model is significant (p=0,000) which means that the variables (genotype and infarction-status) do have an effect on RQ. Looking at each of the variables independently reveals a statistically significant effect on RQ (F=38,086; p=0,000) for the variable infarction-status, as well as a significant effect for the variable genotype (F=17,473; p=0,079). This means that the tested mice show a significantly different RQ value for MMP9 depending on the infarction-status and genotype.

Furthermore, it can be shown that the effect of infarction-status on RQ depends on the genotype because both variables interact significantly (F=14,40; p=0,000).

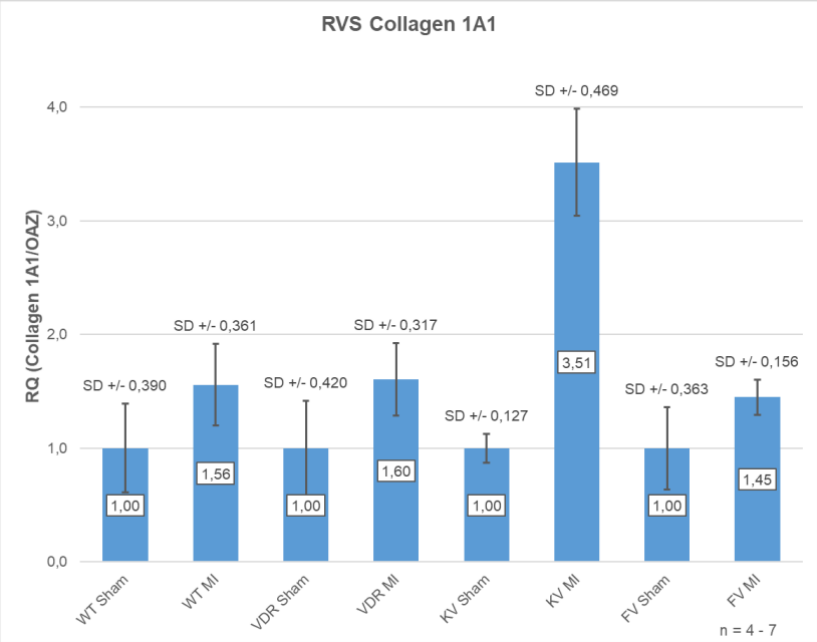

figure 3E: RQ Collagen1A1-OAZ according to infarction-status and genotype

Source	F - value	p - value	partial eta Squared
Corrected Model	2.071	0.071	0.276
Intercept	977.157	0.000	0.963
infarction-status * genotype	1.079	0.370	0.078
infarction-status	12.167	0.001	0.243
genotype	0.425	0.736	0.032
Adjusted R Squared	0.143		

table1E: 2-way ANOVA, gene of interest Collagen1A1

Figure 3E shows the RQ values of collagen 1A1 in the right ventricle and septum for all groups. The results of the multifactorial ANOVA analysis for collagen 1A1 are shown in table 1E. Hereby it can be seen that the overall statistical model is not significant (p=0,071) which means that the variables (genotype and infarction-status) do have no effect on RQ. Looking at each of the variables independently reveals a statistically significant effect on RQ (F=12,167; p=0,001) for the variable infarction-status and no significant effect for the variable genotype (F=0,425; p=0,736). This means that the tested mice show a significantly different RQ value for collagen 1A1 depending on the infarction-status.

Furthermore, it can be shown that the effect of infarction-status on RQ does not depend on the genotype because both variables interact non-significantly (F=1,079; p=0,370).

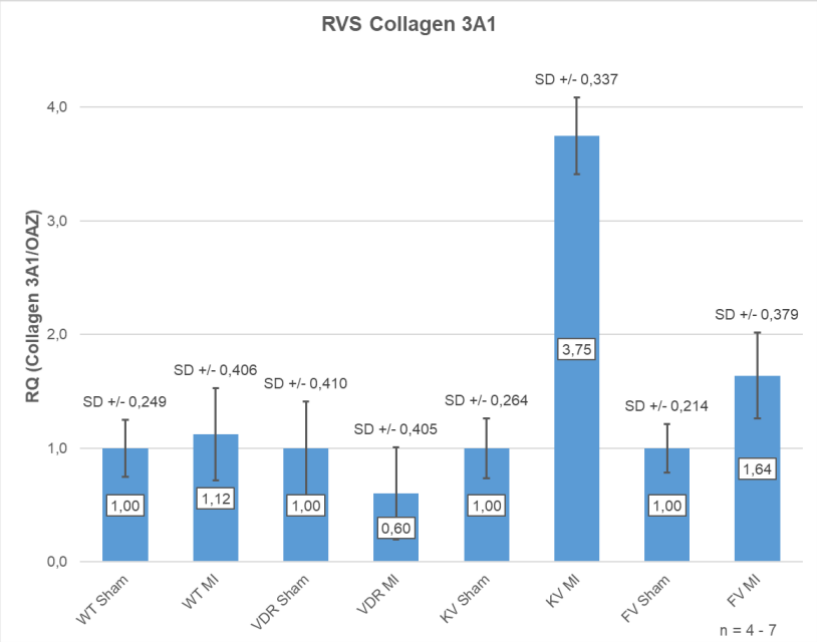

figure 3F: RQ Collagen3A1-OAZ according to infarction-status and genotype

Source	F - value	p - value	partial eta Squared
Corrected Model	3.172	0.010	0.369
Intercept	135.636	0.000	0.781
infarction-status * genotype	4.733	0.007	0.272
infarction-status	4.458	0.041	0.105
genotype	1.077	0.370	0.071
Adjusted R Squared	0.252		

table1F: 2-way ANOVA, gene of interest Collagen3A1

Figure 3F shows the RQ values of collagen 3A1 in the right ventricle and septum for all groups. The results of the multifactorial ANOVA analysis for collagen 3A1 are shown in table 1F. Hereby it can be seen that the overall statistical model is significant (p=0,010) which means that the variables (genotype and infarction-status) do have an effect on RQ. Looking at each of the variables independently reveals a statistically significant effect on RQ (F=4,458; p=0,041) for the variable infarction-status and a non-significant effect for the variable genotype (F=1,077; p=0,370). This means that the tested mice show a significantly different RQ value for MMP9 depending on the infarction-status and genotype.

Furthermore, it can be shown that the effect of infarction-status on RQ depends on the genotype because both variables interact significantly (F=4,733; p=0,007).

Overview figure 4: left ventricle

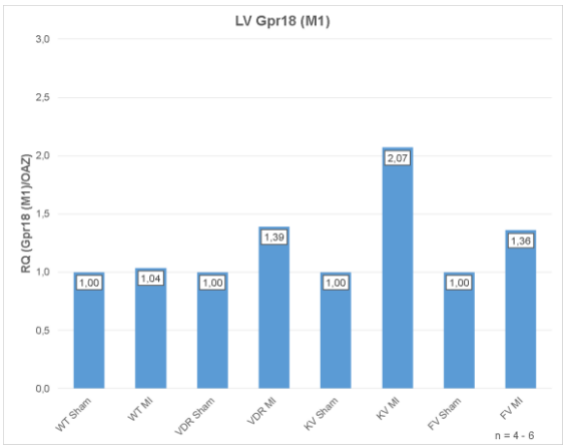

figure 4A

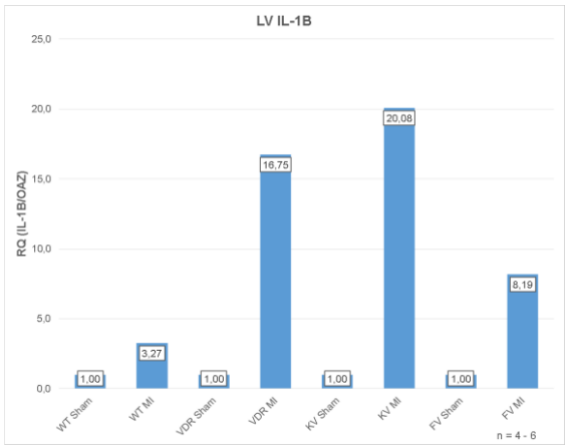

figure 4B

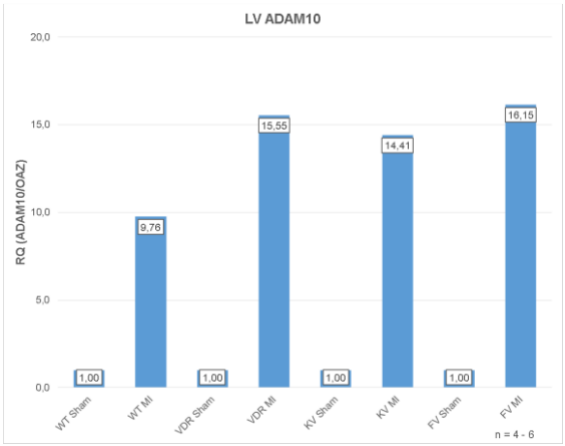

figure 4C

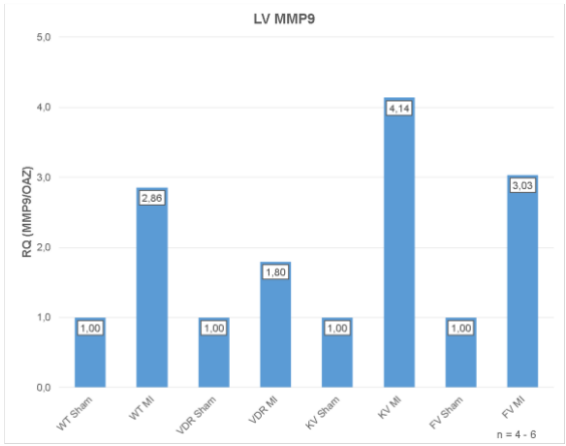

figure 4D

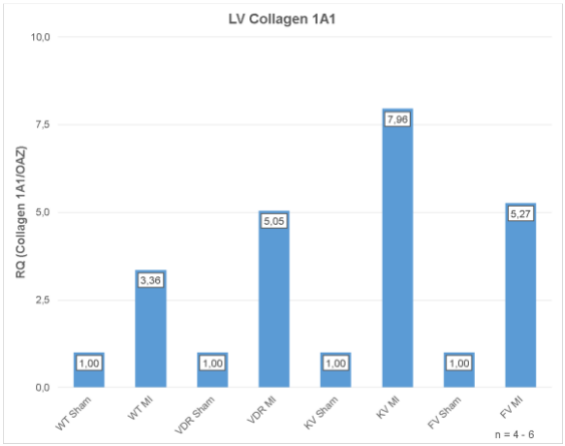

figure 4E

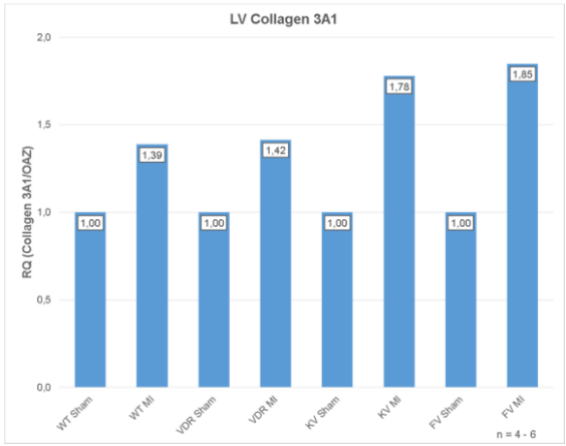

figure 4F

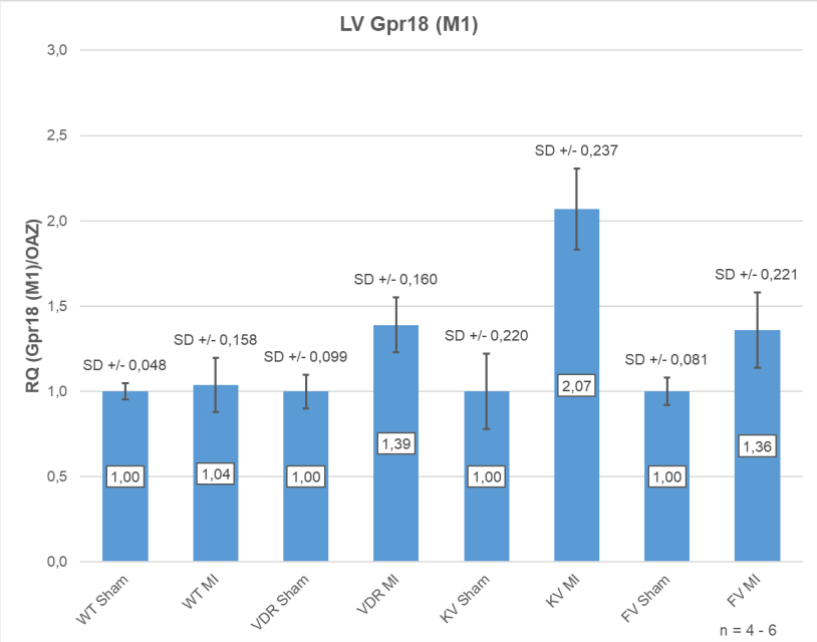

figure 4A: RQ Grp18-OAZ according to infarction-status and genotype

Source	F - value	p - value	partial eta Squared
Corrected Model	4.060	0.002	0.428
Intercept	9,353.340	0.000	0.996
infarction-status * genotype	2.818	0.052	0.182
infarction-status	16.913	0.000	0.308
genotype	0.848	0.476	0.063
Adjusted R Squared	0.323		

table2A: 2-way AVONA, gene of interest Grp18

Figure 4A shows the RQ values of Grp18 in the left ventricle for all groups. The results of the multifactorial ANOVA analysis for Grp18 are shown in table 2A. Hereby it can be seen that the overall statistical model is significant (p=0,002) which means that the variables (genotype and infarction-status) do have an effect on RQ. Looking at each of the variables independently reveals a statistically significant effect on RQ (F=16,913; p=0,000) for the variable infarction-status and a non-significant effect for the variable genotype (F=0,848; p=0,476). This means that the tested mice show a significantly different RQ value for Grp18 depending on the infarction-status.

Furthermore, it can be shown that the effect of infarction-status on RQ does not depend on the genotype because both variables interact non-significantly (F=2,818; p=0,052).

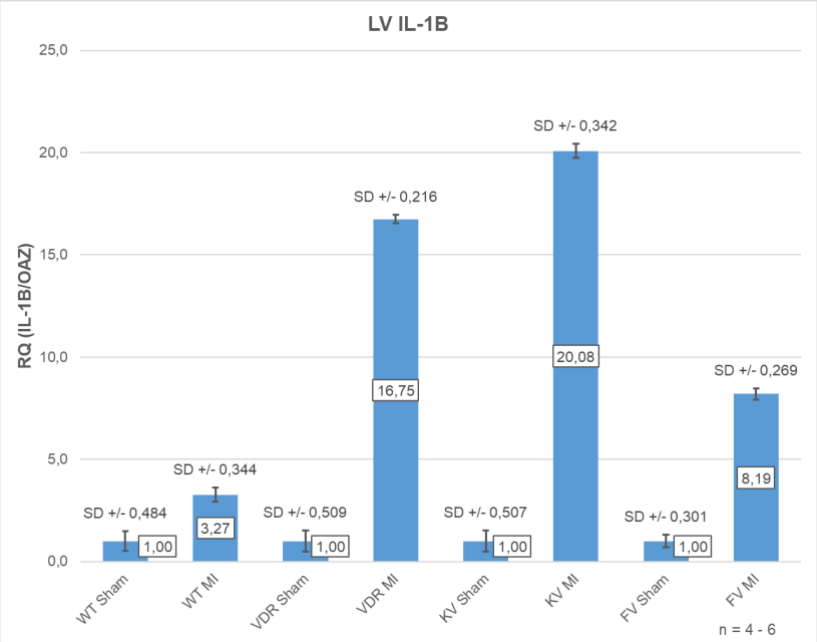

figure 4B: RQ IL-1ß-OAZ according to infarction-status and genotype

Source	F - value	p - value	partial eta Squared
Corrected Model	13.256	0.000	0.72
Intercept	3,527.520	0.000	0.99
infarction-status * genotype	0.926	0.438	0.072
infarction-status	73.413	0.000	0.671
genotype	5.32	0.004	0.307
Adjusted R Squared	0.666		

table2B: 2-way ANOVA, gene of interest IL-1ß

Figure 4B shows the RQ values of IL-1ß in the left ventricle for all groups. The results of the multifactorial ANOVA analysis for IL-1ß are shown in table 2B. Hereby it can be seen that the overall statistical model is significant (p=0,000) which means that the variables (genotype and infarction-status) do have an effect on RQ. Looking at each of the variables independently reveals a statistically significant effect on RQ (F=73,413; p=0,000) for the variable infarction-status as well as for the variable genotype (F=5,32; p=0,004). This means that the tested mice show a significantly different RQ value for IL-1ß depending on the infarction-status and the genotype.

Furthermore, it can be shown that the effect of infarction-status on RQ does not depend on the genotype because both variables interact non-significantly (F=0.926; p=0,438).

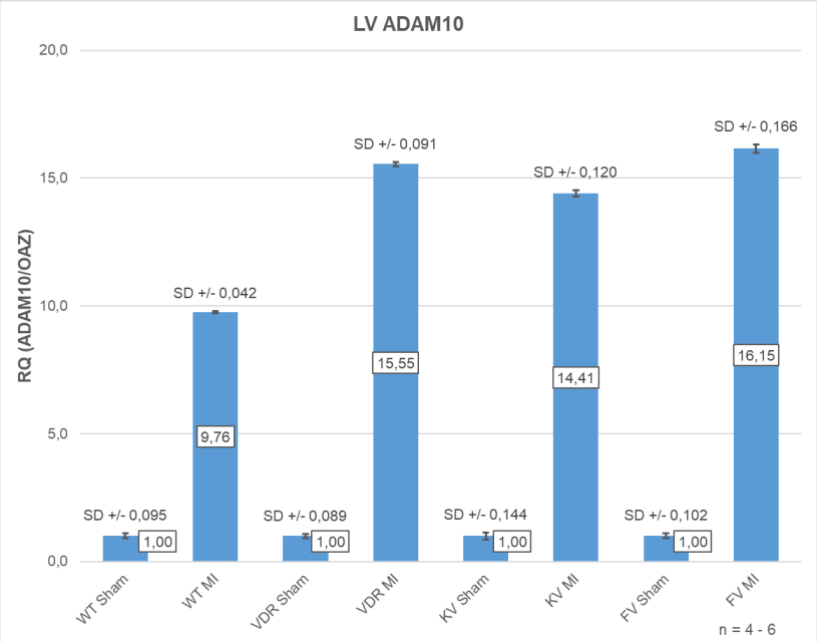

figure 4C: RQ ADAM10-OAZ according to infarction-status and genotype

Source	F - value	p - value	partial eta Squared
Corrected Model	12.028	0.000	0.7
Intercept	2,087.854	0.000	0.983
infarction-status * genotype	1.800	0.165	0.13
infarction-status	70.212	0.000	0.661
genotype	1,870	0.152	135.000
Adjusted R Squared	0.642		

table2C: 2-way ANOVA, gene of interest ADAM10

Figure 4C shows the RQ values of ADAM10 in the left ventricle for all groups. The results of the multifactorial ANOVA analysis for ADAM10 are shown in table 2C. Hereby it can be seen that the overall statistical model is significant (p=0,000) which means that the variables (genotype and infarction-status) do have an effect on RQ. Looking at each of the variables independently reveals a statistically significant effect on RQ (F=70,212; p=0,000) for the variable infarction-status and not a significant effect for the variable genotype (F=1,870; p=0,152). This means that the tested mice show a significantly different RQ value for ADAM10 depending on the infarction-status.

Furthermore, it can be shown that the effect of infarction-status on RQ does not depend on the genotype because both variables interact non-significantly (F=1,800; p=0,165).

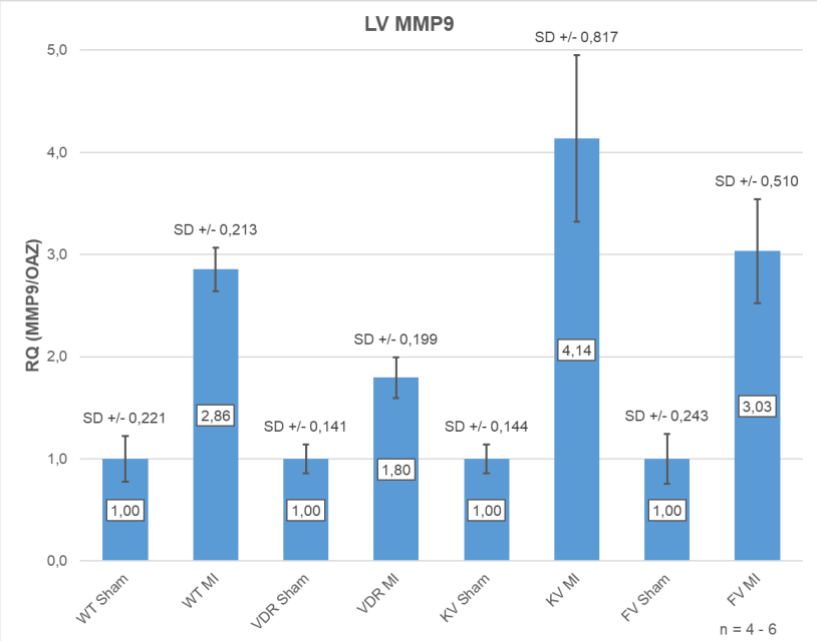

figure 4D: RQ MMP9-OAZ according to infarction-status and genotype

Source	F - value	p - value	partial eta Squared
Corrected Model	4.872	0.001	0.487
Intercept	2,565.164	0.000	0.986
infarction-status * genotype	0.811	0.496	0.063
infarction-status	28.525	0.000	0.442
genotype	0.769	0.519	0.060
Adjusted R Squared	0.387		

table2D: 2-way ANOVA, gene of interest MMP9

Figure 4D shows the RQ values of MMP9 in the left ventricle for all groups. The results of the multifactorial ANOVA analysis for MMP9 are shown in table 2D. Hereby it can be seen that the overall statistical model is significant (p=0,001) which means that the variables (genotype and infarction-status) do have an effect on RQ. Looking at each of the variables independently reveals a statistically significant effect on RQ (F=28,525; p=0,000) for the variable infarction-status and not a significant effect for the variable genotype (F=0,769; p=0,519). This means that the tested mice show a significantly different RQ value for MMP9 depending on the infarction-status but not depending on the genotype.

Furthermore, it can be shown that the effect of infarction-status on RQ does not depend on the genotype because both variables interact non-significantly (F=0,811; p=0,496).

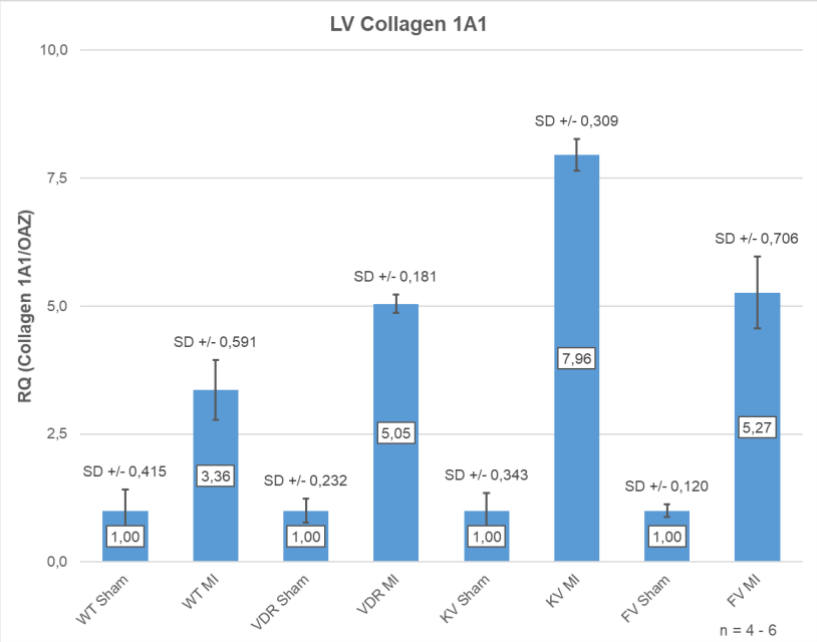

figure 4E: RQ Collagen1A1-OAZ according to infarction-status and genotype

Source	F - value	p - value	partial eta Squared
Corrected Model	21.138	0.000	0.8
Intercept	404.630	0.000	0.916
infarction-status * genotype	4.158	0.012	0.252
infarction-status	120.387	0.000	0.765
genotype	4.161	0.012	0.252
Adjusted R Squared	0.762		

table2E: 2-way ANOVA, gene of interest Collagen1A1

Figure 4E shows the RQ values of collagen 1A1 in the left ventricle for all groups. The results of the multifactorial ANOVA analysis for collagen 1A1 are shown in table 2E. Hereby it can be seen that the overall statistical model is significant (p=0,000) which means that the variables (genotype and infarction-status) do have an effect on RQ. Looking at each of the variables independently reveals a statistically significant effect on RQ (F=120,387; p=0,000) for the variable infarction-status as well as for the variable genotype (F=4,161; p=0,012). This means that the tested mice show a significantly different RQ value for collagen 1A1 depending on the infarction-status and the genotype.

Furthermore, it can be shown that the effect of infarction-status on RQ depends on the genotype because both variables interact significantly (F=4,158; p=0,012).

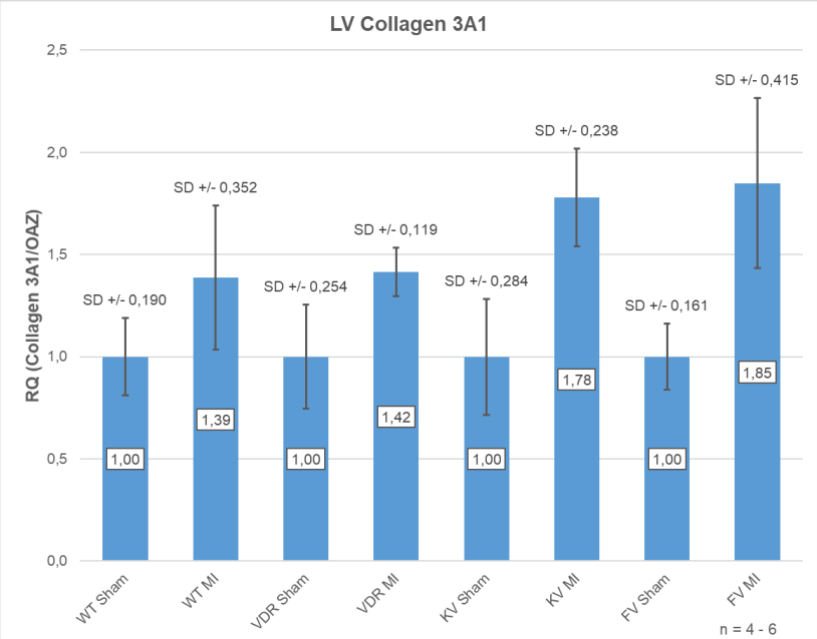

figure 4F: RQ Collagen3A1-OAZ according to infarction-status and genotype

Source	F - value	p - value	partial eta Squared
Corrected Model	66.162	0.000	0.928
Intercept	34.916	0.000	0.492
infarction-status * genotype	0.777	0.515	0.061
infarction-status	422.366	0.000	0.921
genotype	10.053	0.000	0.456
Adjusted R Squared	0.914		

table2F: 2-way ANOVA, gene of interest Collagen3A1

Figure 4F shows the RQ values of collagen 3A1 in the left ventricle for all groups. The results of the multifactorial ANOVA analysis for collagen 3A1 are shown in table 2F. Hereby it can be seen that the overall statistical model is significant (p=0,000) which means that the variables (genotype and infarction-status) do have an effect on RQ. Looking at each of the variables independently reveals a statistically significant effect on RQ (F=422,366; p=0,000) for the variable infarction-status as well as for the variable genotype (F=10,053; p=0,000). This means that the tested mice show a significantly different RQ value for collagen 3A1 depending on the infarction-status and the genotype.

Furthermore, it can be shown that the effect of infarction-status on RQ does not depend on the genotype because both variables interact non-significantly (F=0,777; p=0,515).

4.2 In vitro experiments with cultured cardiac fibroblasts

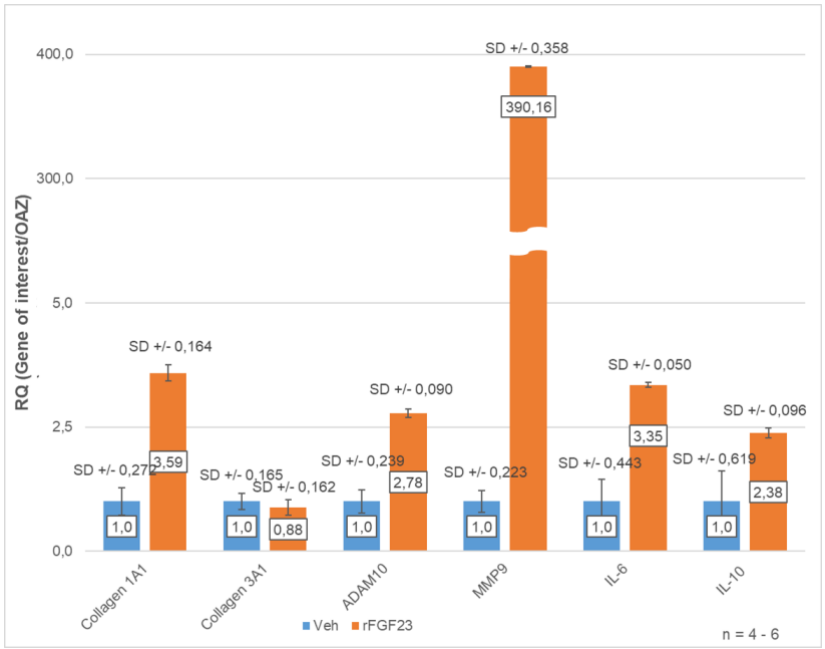

figure 5: RQ Gene of interest-OAZ

Gene of interest	Levene-Test (homogeneity of variance)		T-Test				
	F-value	Sig.	Sig. (2-tailed)	mean difference	std. error difference	lower (95% confidence)	upper (95% confidence)
Collagen 1A1	1.133	0.347	0.004	1.844	0.318	0.961	2.727
Collagen 3A1	0.006	0.940	0.468	-0.185	0.231	-0.827	0.457
ADAM10	4.685	0.096	0.003	1.663	0.256	0.953	2.373
MMP9	1.426	0.298	0.000	8.608	0.422	7.436	9.780
IL-6	12.449	0.024	0.017	1.743	0.445	0.506	2.979
IL-10	8.606	0.043	0.117	1.250	0.626	-0.488	2.989

table 3: t-test for each gene of interest

The t-test shows the following results:

- Collagen 1A1 shows a significant difference (p=0,004) between Veh and rFGF 23 regarding the RQ-value, with homogeneous variances (F-test: p=0,347).
- Collagen 3A1 shows no significant difference (p=0,468) between Veh and rFGF 23 regarding the RQ-value, with homogeneous variances (F-test: p=0,940).

- ADAM10 shows a significant difference (p=0,003) between Veh and rFGF 23 regarding the RQ-value, with homogeneous variances (F-test: p=0,096).
- MMP9 shows a significant difference (p=0,000) between Veh and rFGF 23 regarding the RQ-value, with homogeneous variances (F-test: p=0,298).
- IL-6 shows no significant difference (p=0,057) between Veh and rFGF 23 regarding the RQ-value, with inhomogeneous variances (F-test: p=0,024).
- IL-10 shows no significant difference (p=0,178) between Veh and rFGF 23 regarding the RQ-value, with inhomogeneous variances (F-test: p=0,043).

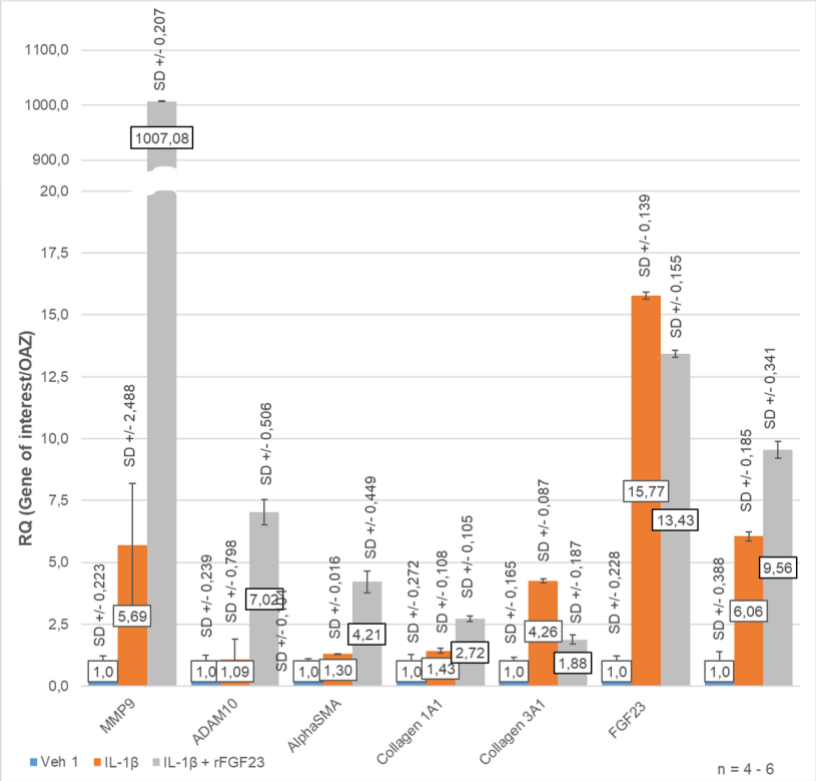

figure 6: RQ gene of interest-OAZ

Gene of Interest		Sum of Squares	df	Mean Square	F	Sig.
MMP9	Between Groups	161.580	2	80.790	12.858	0.007
	Within Groups	37.701	6	6.283		
	Total	199.281	8			
ADAM10	Between Groups	15.136	2	7.568	7.968	0.020
	Within Groups	5.699	6	0.950		
	Total	20.835	8			
Alpha SMA	Between Groups	7.328	2	3.664	17.207	0.003
	Within Groups	1.278	6	0.213		
	Total	8.606	8			
Collagen 1A1	Between Groups	3.212	2	1.606	16.885	0.004
	Within Groups	0.582	6	0.097		
	Total	3.794	8			
Collagen 3A1	Between Groups	6.589	2	3.295	47.211	0.000
	Within Groups	0.419	6	0.070		
	Total	7.008	8			
FGF 23	Between Groups	29.930	2	14.965	157.053	0.000

	Within Groups	0.572	6	0.095		
	Total	30.502	8			
	Between Groups	17.794	2	8.897	29.541	0.001
Klotho	Within Groups	1.807	6	0.301		
	Total	19.601	8			

table 4: 1-way ANOVA gene of interest

The analysis of variance carried out in figure 6 (one-way ANOVA) shows a significant result for all genes of interest. Consequently, the RQ- values of the different groups (represented by different treated cells: Veh, IL-1ß and IL-1ß+rFGF23) differ significantly from one another for each gene of interest. A post-hoc test (LSD) for homogeneous variances was carried out for the individual genes, which shows the following results:

- For MMP9 there is no significant difference between Veh and IL-1ß (p=0,266). IL-1ß+rFGF23 is significantly different from the other two treatments.
- For ADAM10 there is no significant difference between Veh and IL-1ß (p=0,879). IL-1ß+rFGF23 is significantly different from the other two treatments.
- For AlphaSMA there is no significant difference between Veh and IL-1ß (p=0,359). IL-1ß+rFGF23 is significantly different from the other two treatments.
- For collagen 1A1 there is no significant difference between Veh and IL-1ß (p=0,359). IL-1ß+rFGF23 is significantly different from the other two treatments.
- For collagen 3A1 there is a significant difference between all groups.
- For FGF 23 there is no significant difference between IL-1ß and IL-1ß+rFGF23 (p=0,392). Veh is significantly different from the other two treatments.
- For Klotho there is no significant difference between IL-1ß and IL-1ß+rFGF23 (p=0,192). Veh is significantly different from the other two treatments.

5 Discussion

To answer the research questions, the two experiments should be reviewed separately. In order to answer the question if FGF 23 does trigger an inflammatory response after MI, it is necessary to take a closer look at the organ level, where the right ventricle and septum is compared to the left ventricle. It could be clearly illustrated that FGF 23 intensifies the inflammatory response, represented by the significantly lower expression of IL-1ß in FV and KV animals in non-ischemic tissue. Interestingly, the difference in IL-1ß expression between the different genotypes are not that clearly visible after MI. When taking a closer look at the results in the left ventricle, there is mainly a difference between the animals in which an AMI was triggered by surgery (MI) and those in which no AMI was triggered (Sham), regardless of which genotype they belong to. This leads to the assumption that FGF 23 increases a pro-inflammatory response in healthy non-ischemic tissue but does not trigger it per se after a myocardial infarction. The situation is similar when focusing on the expression of MMP9 and ADAM 10 in the different tissues. While FGF 23 appears to increase the expression of MMP9 and ADAM 10 in healthy tissue and thus influence the collagen regulation, the situation is different in the left ventricle. As expected, a clear difference between Sham and MI mice can be seen but there is no significant difference between the individual genotypes. Additionally, this experiment already shows very clearly that FGF 23 seems to promote collagen production in a Klotho dependent manner after myocardial infarction.

In summary, it can be said that, firstly FGF 23 increases a pro-inflammatory response and regulates collagen by increasing MMP9 and ADAM10 expression in the absence of a pro-inflammatory stimulus. Secondly, after the activation of a proinflammatory pathway, specifically a myocardial infarction in this context, FGF 23 seems to stimulate collagen type 1 activity.

Very similar results could also be observed in study performed in 2016 (HUIXNIN et al., 2016), which showed that FGF 23 can induce myocardial fibrosis, which underlines the results observed in this investigation.

Moreover, if we take a closer look at cellular levels, the situation becomes even more specific. The second experiment revolves around the question of whether FGF 23 stimulates collagen deposition after AMI. In order to answer the second research question, we used isolated fibroblasts to show the influence of recombinant FGF 23 (rFGF 23) on these cells (figure 3) and to compare the influence of a pro-inflammatory stimulus, represented by fibroblasts treated

with IL-1ß, and a pro-inflammatory stimulus in combination with rFGF 23 (IL-1ß+rFGF 23) on fibroblasts (figure 6).

The results demonstrate that FGF 23 increases collagen production and stimulates collagen regulation, as fibroblast treated with rFGF 23 show significantly higher expression of MMP9, ADAM 10 and collagen type 1, compared to untreated cells. Nonetheless, the initially assumed pro-inflammatory effect, represented by IL-6 expression, as well as anti-inflammatory effect, visualized by IL-10 expression, of FGF 23 could not be confirmed in this experiment. This observation clarifies that the effect of FGF 23 on collagen is driven through fibroblasts and is independent of a pro-inflammatory stimulus. In addition, there are indications that the fibroblast proliferation is promoted by FGF 23 and is dependent on exposure time and FGF 23 concentrations.

Additionally, the fibroblasts treated with IL-1ß were compared to vehicle treated cells and to fibroblasts, which were treated with a combination of IL-1ß and rFGF23, to visualize the difference between a pro-inflammatory stimulus and a FGF 23 induced scenario in these cells. It is very exciting to see that the pro-inflammatory response increases FGF 23, shown by elevated FGF 23 concentrations in fibroblasts treated with IL-1ß, and that only the co-treatment of IL-1ß and rFGF23 seems to stimulate collagen deposition. This assumption is based on the fact that the co-treatment with IL-1ß and rFGF23 leads to elevated MMP9, ADAM10 and collagen type 1 expression in fibroblasts, while cells only treated with IL-1ß do not show this effect. Interestingly, it seems that collagen type 3 expression increased through elevated IL-1ß levels, while FGF 23 seems to not have an influence on the production of collagen type 3.

6 Conclusion

The aim of the study was to provide insights into the molecular changes after a myocardial infarction. Overall, this has been achieved through the experiments mentioned above. The FGF 23 induced scenarios appear to be complex and some questions remain open for further investigations.

In order to summarize the observed events, the following statements can be made:

FGF 23 increases a pro-inflammatory response, promotes collagen deposition and increases collagen production in non-ischemic tissue. This observation suggests that FGF 23 is increased by other unknown stimuli, but appears to play an important role in inflammatory response as it intensifies the reaction. Interestingly, this cannot be seen in ischemic tissue. After activation of a pro-inflammatory pathway, represented by a myocardial infarction, the molecular changes do not differ significantly between the mice of different genotypes. This could possibly be explained by the assumption that the effects of FGF 23 are oxygen dependent or that other control regulations suppress FGF 23 interactions after myocardial infarction.

In addition, the effect of FGF 23 on fibroblasts could be illustrated. The investigations show that FGF 23 has an influence on fibroblasts and is significantly involved in ECCM formation. It is very interesting to see the different influences on fibroblasts in comparison to each other. It is clearly shown that an inflammatory reaction increases FGF 23 in fibroblast. At this point it should be clarified, that in the second part of the experiment, in which everything revolves around the reaction at the cellular level, no distinction is made between ischemic and non-ischemic conditions. Also, a possible oxygen-dependent influence on the effect of FGF 23 cannot be ruled out in this experiment. Another very exciting observation is that a pro-inflammatory response seems to not have an effect on collagen deposition, whereas a FGF 23, as well as a co-treatment with IL-1ß and rFGF 23 stimulates collagen deposition. Therefore, it can be concluded that a pro-inflammatory stimulus increases FGF 23 concentrations and that the effect of FGF 23 on collagen is driven through fibroblasts, while a pro-inflammatory stimulus per se does not have an effect on collagen deposition.

To summarize the findings, the initial situation in mammalian bodies should be described first. As a starting point in this scenario we need to have a closer look at the ischemic tissue, which is caused by myocardial infarction more often than not. Myocardial infarction is a condition leading to ischemic heart diseases due to a blood clot in an arteriosclerotic altered constriction

of a coronary artery. The main task of coronary arteries is to supply the blood to cardiac muscle cells and to provide oxygen which is necessary for proper physiological function of the heart. When oxygen is no longer transported due to such local circulatory disorders in the heart muscle, cardia muscle cells undergo cell death. Although the adult mammalian heart cannot rebuild new muscle cells in response to injury, myocardial repair is triggered by cytokines released from necrotic myocytes. One of these cytokines is Transforming growth factor $_1$ which is responsible for fibroblast chemotaxis and fibroblasts proliferation from fibroblasts to myofibroblasts, which are able to synthesis collagen type 1 and type 3.

Additionally, it is known that some members of the FGF family are able to induce fibrosis in different tissues and that fibroblast growth factor 23 do have a cardiac effect as it induces directly left ventricular hypertrophy (FAUL et al., 2011). This led to the hypothesis that fibroblast growth factor 23 is a regulator of inflammation and collagen deposition during ischemic heart disease. It is remarkable that cardiac hypertrophy is also a risk factor for ischemic heart diseases, which can potentially result in a vicious circle.

If the mentioned observations are combined, the following scenario can be assumed: it is possible that necrotic myocardial muscle cells release Interleukin- and Transforming growth factor $_1$, which we know induces the transformation from fibroblast to myofibroblasts (BODH, 2003). The pro-inflammatory stimulus, represented by a myocardial infarction in this specific context, increases FGF 23. FGF 23 acts directly on fibroblasts, shows the tendency to promote fibroblast proliferation and causes collagen deposition due to an increase in MMP9, ADAM10 and collagen type 1 concentrations. Therefore, it seems that the role of FGF 23 in inflammation is to stimulate fibroblasts, which respond with collagen type 1 production and an activation of collagen regulators.

While this study shows an overview of the molecular changes in various tissue models after myocardial infarction, it leaves room for further investigations in order to manifest new therapeutic approaches in ischemic heart disease patients.

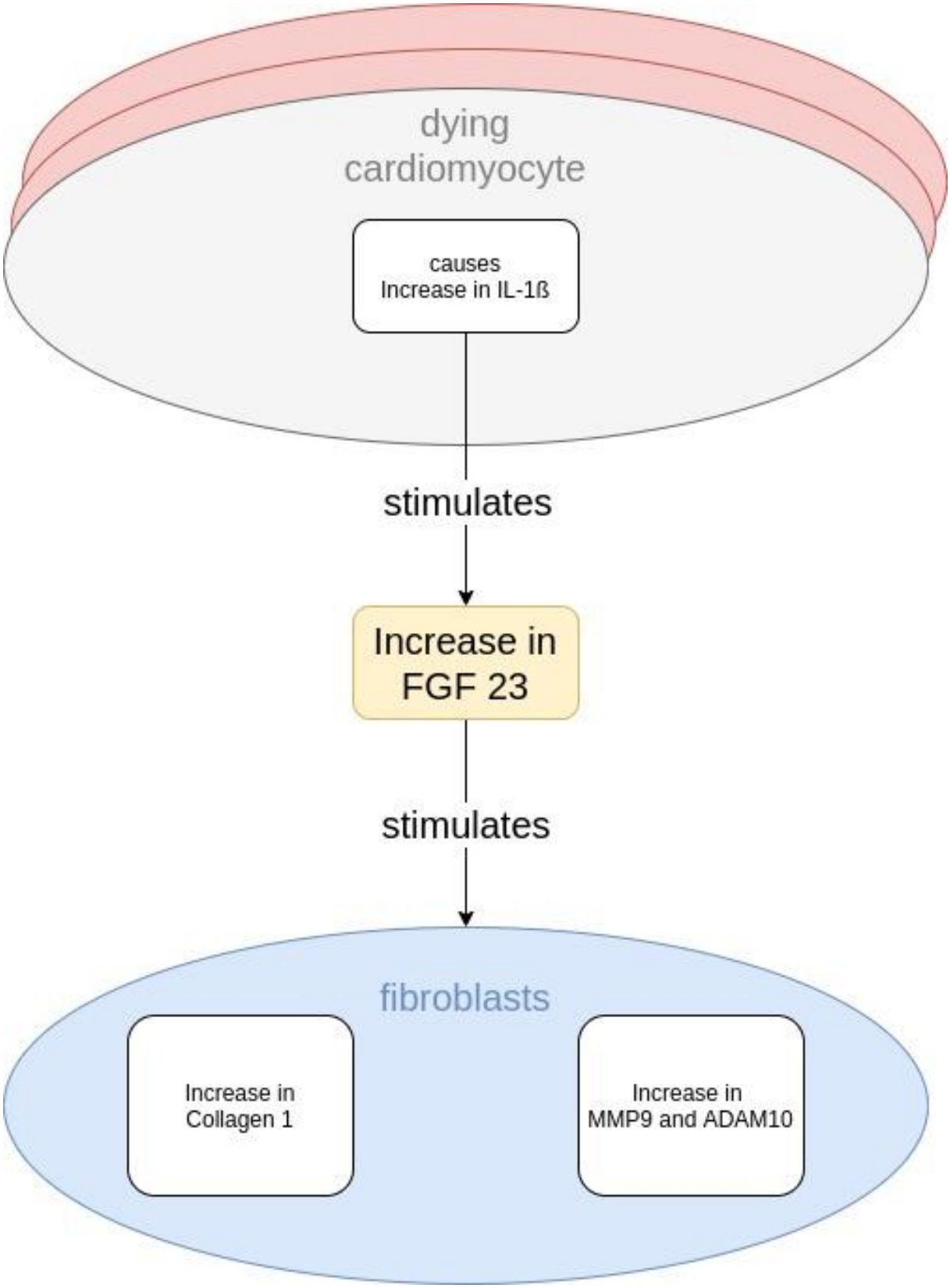
dying
cardiomyocyte
causes
Increase in IL-1ß
stimulates
Increase in
FGF 23
stimulates
fibroblasts
Increase in
Collagen 1
Increase in
MMP9 and ADAM10

6.1 Recommendations and suggestions for further research

This study offers promising approaches to understand the pathological mechanism after a myocardial infarction, but further investigations are necessary and recommended in order to fully understand the events and to develop possible new therapies.

On one hand, as already mentioned, it would be interesting to focus specifically on the situation in ischemic-tissue. Moreover, the events in the left ventricle raise new questions and it would be useful to confirm whether the assumption can be verified that the FGF 23 induced actions are potentially oxygen-dependent. To answer these questions, the investigations carried out on fibroblasts could also be applied to the ischemic tissue. If they take place under the same conditions, they could be compared with the results presented in this work and could possibly provide further information.

On the other hand, the demonstrated results and the already known observation that FGF 23 induces left ventricular hypertrophy independent of kidney function, lead to further research questions. For example it is possible that left ventricular hypertrophy is not caused by hypertension but by the changes in the ECCM, as a result the effects of FGF 23 described in this work. In order to explain it in more detail, it is necessary to take a closer look at the physiological mechanisms in the heart.

Furthermore, this study has drawn another conclusion that can be better explained with the “Frank-Starling principle”. This principle describes the ability of the heart to respond to stretching of the tissue, induced by a larger amount of blood volume, with increased stroke volume (NETTER, in BECKER and PILGRIM, 2000). Through fibrosis of the tissue its elasticity decreases, the “Frank-Starling principle” can no longer function adequately and maybe over time volume overload occurs, leading to hypertrophy of the heart muscle. This study has shown that the fibrosis of the tissue was promoted by the increased production of collagen type 1, induced by FGF 23. This result raises exciting new questions, and offers the opportunity for further extensive investigations.

7 Bibliography

AMOUR, A., KNIGHT, C. G., WEBSTER, A., SLOCOMBE, P. M., STEPHENS, P. E., KNÄUPER, V., DOCHERTY, A. J. P., MURPHY, G. (2000): The in virto activity of ADAM-10 is inhibited by TIMP-1 and TIMP-3. FEBS Letters **473**: 275-279.doi10.1016/s0014-5793(00)01528-3.

ANTMAN, E. M., LOSCALZO, J. (2012): ST-Segment Elevation Myocardial Infarction. In: LONGO, D. L. et al (Editor):Harrison's principles of internal medicine. Vol. 2,18th Edition, The McGraw-Hill Companies, USA, 2021-2034.

BAUM, J., DUFFY, H. S. (2011): Fibroblasts and Myofibroblasts: What are we talking about?. J Cardiovasc Pharmacol **57**(4):376-379. doi:10.1097/FJC.0b013e3182116e39.

BELL, R. M., MOCANU, M. M., YELLON, D. M. (2011): Retrograde heart perfusion: The Langendorff technique of isolated heart perfusion. Journal of Molecular and Cellular Cardiology **50**: 940-950. doi:10.1016/j.yjmcc.2011.02.018.

BODH, I. J. (2003): Ventricular Remodeling After Infarction and the Extracellular Collagen Matrix When Is Enough Enough?. Circulation **108**: 1395-1403. doi:10.1161/01.CIR.0000085658.98621.49.

CHERNG, S., YOUNG, J., MA, H. (2008): Alpha-Smooth Muscle Actin (. The journal of American Science **4** (4), ISSN 1545-1033.

DAVID, V., FRANCIS, C., BABITT, J. L. (2016): Ironing out the crosstalk between FGF23 and inflammation. Am J Physiol Renal Physiol(August 31, 2016).doi:10.1152/ajprenal.00359.2016.

DRIEHUYS, S. et al. (1998): Myocardial Infarction in dogs and cats: 37 cases (1985-1994), J. American Vet. Med Association **213** (10),1444-1448.

ERBEN, R. G., SOEGIARTO, D. W., WEBER, K., ZEITZ, U., LIEBERHERR, M., GNIADECKI R, et al. (2002): Deletion of deoxyribonucleic acid binding domain of the vitamin D receptor abrogates genomic and nongenomic functions of vitamin D. Mol Endocrinol **16**: 1524–37. https://doi.org/10.1210/mend.16.7.0866 PMID: 12089348

FAUL, C., AMARAL, A. P., OSKOUEI, B. (2011): FGF23 induces left ventricular hypertrophy. J Clin invest **121**(11),4393-4408.doi:10.1172/JCI46122.

FAUL, C. (2016): Cardiac actions of fibroblast growth factor 23. Bone (2016), http://dx.doi.org/10.1016/j.bone.2016.10.001.

FORD, K., LATIC, N., SLAVIC, S., ZEITZ, U., DOLEZAL, M., ANDRUKHOV, O., ERBEN, R. G., ANDRUKHOVA, O. (2018): Lack of vitamin D signaling per se does not aggravate cardiac functional impairment induced by myocardial infarction in mice. PLOS ONE **13** (10):e0204803.https://doi.org/10.1371/journal.pone.0204803.

GAZIANO, T. A., GAZIANO J. M. (2012): Epidemiology of Cardiovascular Disease. In: LONGO, D. L. et al (Editor):Harrison's principles of internal medicine. Vol. 2,18th Edition, The McGraw-Hill Companies, USA, 1811-1816.

GRAHAM, E. L., BALLA, C., FRANCHINO, H., MELMAN, Y., DEL MONTE, F., DAS, S. (2013): Isolation, Culture, and Functuional Characterization of Adult Mouse Cardiomyocytes. J. Vis. Exp. (79), e50289, doi:10.3791/50289.

GROS, G. (2010): Atmung. In: von Engelhardt, W. (Editor): Physiologie der Haustiere. Vol. 3, Enke Verlag, Stuttgart, 241-280.

GRUBER, A. D. et al (2002): Atherosclerosis with multifocal myocardial infarction in a Pacific calrus, Journalof zoo and wildlife medicine: official publication of the American Association of Zoo Veterinarians **2** (3), 139-144.doi.org/10.1638/1042.

HAFFNER, D., LEIFHEIT-NESTLER, M. (2016): Extrarenal effects of FGF 23. Springer Educational Review.doi10.1007/s00467-016-3505-3.

HARMEYER, J., TOBIAS, R. (2010): Herz. In: von Engelhardt, W. (Editor): Physiologie der Haustiere. Vol. 3, Enke Verlag, Stuttgart, 141-173.

HUIXIN, H., XIXIAN, L., QINGMAN, L. et al. (2016): FGF23 promotes myocardial fibrosis in mice through activation of catenin. Oncotarget, Advance Publications (2016).

LOUCH, W. E., SHEEHAN, K. A., WOLSKA, B. M. (2011): Methods in Cardiomyocyte Isolation, Culture and Gene Transfer. J Mol Cell Cardiol **5**1 (3): 288-298.doi:10.1016/j.yjmcc.2011.06.012.

MANN, D. L., CHAKINALA, M. (2012): Heart Failure and Cor Pulmonale. In: LONGO, D. L. et al (Editor):Harrison's principles of internal medicine. Vol. 2,18th Edition, The McGraw-Hill Companies, USA, 1901-1915.

MARIAN, B. (2007): Krankheiten, Krankheitsursachen und -bilder. Facultas Universitätsverlag, 1st Edition.

NETTER, F. H. (2000): Koronare Herzkrankheit. In: Becker, M., Pilgrim, T. (Editors): Netters Innere Medizin. Gerog Thieme Verlag, Stuttgart, 26-43.

NETTER, F. H. (2000): Erworbene Herzklappenfehler. In: Becker, M., Pilgrim, T. (Editors): Netters Innere Medizin. Gerog Thieme Verlag, Stuttgart, 72-93.

RICH, L. , WHITTAKER, P. (2005): Collagen and Picrosirius red stainig: a polarized light assessment of fibrillar hue and spatial distribution. Braz. J. morphol Sci., **22** (2).

ROSSAINT, J., OEHMICHEN, J., VAN AKEN, H. REUTER, S., PAVENSTADT, HJ., MEERSCH, M., UNRUH, M., ZARBOCK, A. (2016): FGF23 signaling impairs neutrophil recruitment and host defense during CKD. J Clin Invest **126**:962-974.

SUTTON, M. G. St. J., SHARPE, N. (2000): Left Ventricular Remodeling After Myocardial Infarction Pathophysiology and Therapy. Circulation. 2000; 101: 2981-2988.

TAKENOUCHI, R., INOUE, K., KAMBE, Y., MIYATA, A. (2012): N-arachidonoyl glycine induces macrophage apoptosis via GPR18. Biochemical and Biophysical Research Communications. Elsevier **418** (2): 366-371.https://doi1,org/0.1016/j.bbrc.2012.01.027.

XIN, M., OLSON, E. N., BASSEL-DUBY, R. (2013): Mending broken heart: cardiac development as a basis for adult heart regeneration and repair. In: Macmillan Publishers Limited: Nature Reviews, Molecular cell Biology (August 2013), Vol. 14, 529-541. doi.10.1038/nrm3619.

Web sources:

APPLIED BIOSYSTEMS (2010): TRI Reagent Solution RNA/DNA/Protein Isolation Reagent. Ambion, Inc. http://www.appliedbiosystems.com.

APPLIED BIOSYSTEMS (2011): Real-time RCR: Understanding C_t. life technologies.http://www.lifetechnologies.com

Bundes rztekammer (B K), Kassen rztliche Bundesvereinigung (KBV), Arbeitsgemeinschaft der Wissenschaftlichen Medizinischen Fachgesellschaften (AWMF). Nationale VersorgungsLeitlinie Chronische KHK – Langfassung, 5th edition. Version 1. 2019 [cited: 2019.07.01]. DOI: 10.6101/AZQ/000419. www.khk.versorgungsleitlinien.de.

Bundesministerium für Soziales, Gesundheit, Pflege und Konsumentenschutz. https://www.sozialministerium.at/cms/site/attachments/8/7/1/CH4052/CMS1421311013881/hke_bericht_2015.pdf, last access: 13.07.2019.

ALBES, J., BUTTER C., (2019): Anatomie des Herzens

https://herzzentrum.immanuel.de/ratgeber/herz-vorsorge/anatomie-des-herzens/, last access: 13.07.2019.

Promega Analysis Notebook. Quantifying RNA with qRT-PCR. http://www.promega.com

STATISTIK AUSTRIA.
https://www.statistik.at/web_de/statistiken/menschen_und_gesellschaft/gesundheit/todesursachen/todesursachen_im_ueberblick/index.html, last access: 13.07.2019.

List of tables

Figure 3:

Tests der Zwischensubjekteffekte[a]

Abhängige Variable: dCT dCT

Quelle	Quadratsumme vom Typ III	df	Mittel der Quadrate	F	Sig.	Partielles Eta-Quadrat
Korrigiertes Modell	3,647[b]	7	,521	5,407	,000	,513
Konstanter Term	82,147	1	82,147	852,585	,000	,959
Art * Maus	1,289	3	,430	4,460	,009	,271
Art	1,689	1	1,689	17,525	,000	,327
Maus	,710	3	,237	2,457	,079	,170
Fehler	3,469	36	,096			
Gesamt	98,278	44				
Korrigierte Gesamtvariation	7,116	43				

a. Gen Gen = ADAM10

b. R-Quadrat = ,513 (korrigiertes R-Quadrat = ,418)

Tests der Zwischensubjekteffekte[a]

Abhängige Variable: dCT dCT

Quelle	Quadratsumme vom Typ III	df	Mittel der Quadrate	F	Sig.	Partielles Eta-Quadrat
Korrigiertes Modell	6,565[b]	7	,938	2,298	,047	,297
Konstanter Term	2547,175	1	2547,175	6242,238	,000	,994
Art * Maus	2,982	3	,994	2,436	,080	,161
Art	2,354	1	2,354	5,770	,021	,132
Maus	1,746	3	,582	1,426	,250	,101
Fehler	15,506	38	,408			
Gesamt	2790,522	46				
Korrigierte Gesamtvariation	22,071	45				

a. Gen Gen = Gpr18 (M1)

b. R-Quadrat = ,297 (korrigiertes R-Quadrat = ,168)

Tests der Zwischensubjekteffekte[a]

Abhängige Variable: dCT dCT

Quelle	Quadratsumme vom Typ III	df	Mittel der Quadrate	F	Sig.	Partielles Eta-Quadrat
Korrigiertes Modell	65,203[b]	7	9,315	6,489	,000	,558
Konstanter Term	2018,891	1	2018,891	1406,532	,000	,975
Art * Maus	12,509	3	4,170	2,905	,048	,195
Art	39,999	1	39,999	27,867	,000	,436
Maus	21,025	3	7,008	4,883	,006	,289
Fehler	51,673	36	1,435			
Gesamt	2301,333	44				
Korrigierte Gesamtvariation	116,876	43				

a. Gen Gen = IL-1B

b. R-Quadrat = ,558 (korrigiertes R-Quadrat = ,472)

Tests der Zwischensubjekteffekte[a]

Abhängige Variable: dCT dCT

Quelle	Quadratsumme vom Typ III	df	Mittel der Quadrate	F	Sig.	Partielles Eta-Quadrat
Korrigiertes Modell	10,791[b]	7	1,542	2,071	,071	,276
Konstanter Term	727,387	1	727,387	977,157	,000	,963
Art * Maus	2,409	3	,803	1,079	,370	,078
Art	9,057	1	9,057	12,167	,001	,243
Maus	,949	3	,316	,425	,736	,032
Fehler	28,287	38	,744			
Gesamt	837,110	46				
Korrigierte Gesamtvariation	39,077	45				

a. Gen Gen = Col1A1

b. R-Quadrat = ,276 (korrigiertes R-Quadrat = ,143)

Tests der Zwischensubjekteffekte[a]

Abhängige Variable: dCT dCT

Quelle	Quadratsumme vom Typ III	df	Mittel der Quadrate	F	Sig.	Partielles Eta-Quadrat
Korrigiertes Modell	340,511[b]	7	48,644	16,499	,000	,752
Konstanter Term	1222,799	1	1222,799	414,739	,000	,916
Art * Maus	127,405	3	42,468	14,404	,000	,532
Art	112,292	1	112,292	38,086	,000	,501
Maus	154,550	3	51,517	17,473	,000	,580
Fehler	112,038	38	2,948			
Gesamt	1901,921	46				
Korrigierte Gesamtvariation	452,549	45				

a. Gen Gen = MMP9

b. R-Quadrat = ,752 (korrigiertes R-Quadrat = ,707)

Leven-Test Fig. 1 F	**df1**	**df2**	**Sig.**
ADAM10	1,786	7	36	0,120
Col1A1	2,051	7	38	0,074
Collagen 3	0,804	7	38	0,589
Gpr18 (M1)	1,305	7	38	0,274
IL-1B	2,434	7	36	0,058
MMP9	2,887	7	38	0,056

Figure 4:

Tests der Zwischensubjekteffekte[a]

Abhängige Variable: dCT dCT

Quelle	Quadratsumme vom Typ III	df	Mittel der Quadrate	F	Sig.	Partielles Eta-Quadrat
Korrigiertes Modell	170,653[b]	7	24,379	66,163	,000	,928
Konstanter Term	12,865	1	12,865	34,916	,000	,492
Art * Maus	,859	3	,286	,777	,515	,061
Art	155,629	1	155,629	422,366	,000	,921
Maus	11,113	3	3,704	10,053	,000	,456
Fehler	13,265	36	,368			
Gesamt	198,433	44				
Korrigierte Gesamtvariation	183,918	43				

a. Gen Gen = Collagen 3A1

b. R-Quadrat = ,928 (korrigiertes R-Quadrat = ,914)

Tests der Zwischensubjekteffekte[a]

Abhängige Variable: dCT dCT

Quelle	Quadratsumme vom Typ III	df	Mittel der Quadrate	F	Sig.	Partielles Eta-Quadrat
Korrigiertes Modell	29,429[b]	7	4,204	4,872	,001	,487
Konstanter Term	2213,314	1	2213,314	2565,164	,000	,986
Art * Maus	2,098	3	,699	,811	,496	,063
Art	24,613	1	24,613	28,525	,000	,442
Maus	1,991	3	,664	,769	,519	,060
Fehler	31,062	36	,863			
Gesamt	2290,873	44				
Korrigierte Gesamtvariation	60,491	43				

a. Gen Gen = MMP9

b. R-Quadrat = ,487 (korrigiertes R-Quadrat = ,387)

Tests der Zwischensubjekteffekte[a]

Abhängige Variable: dCT dCT

Quelle	Quadratsumme vom Typ III	df	Mittel der Quadrate	F	Sig.	Partielles Eta-Quadrat
Korrigiertes Modell	5,924[b]	7	,846	12,028	,000	,700
Konstanter Term	146,896	1	146,896	2087,854	,000	,983
Art * Maus	,380	3	,127	1,800	,165	,130
Art	4,940	1	4,940	70,212	,000	,661
Maus	,395	3	,132	1,870	,152	,135
Fehler	2,533	36	,070			
Gesamt	156,579	44				
Korrigierte Gesamtvariation	8,457	43				

a. Gen Gen = ADAM10

b. R-Quadrat = ,700 (korrigiertes R-Quadrat = ,642)

Tests der Zwischensubjekteffekte[a]

Abhängige Variable: dCT dCT

Quelle	Quadratsumme vom Typ III	df	Mittel der Quadrate	F	Sig.	Partielles Eta-Quadrat
Korrigiertes Modell	4,906[b]	7	,701	4,060	,002	,428
Konstanter Term	1614,572	1	1614,572	9353,340	,000	,996
Art * Maus	1,459	3	,486	2,818	,052	,182
Art	2,920	1	2,920	16,913	,000	,308
Maus	,439	3	,146	,848	,476	,063
Fehler	6,560	38	,173			
Gesamt	1630,840	46				
Korrigierte Gesamtvariation	11,466	45				

a. Gen Gen = Gpr18 (M1)

b. R-Quadrat = ,428 (korrigiertes R-Quadrat = ,323)

Tests der Zwischensubjekteffekte[a]

Abhängige Variable: dCT dCT

Quelle	Quadratsumme vom Typ III	df	Mittel der Quadrate	F	Sig.	Partielles Eta-Quadrat
Korrigiertes Modell	73,612[b]	7	10,516	13,256	,000	,720
Konstanter Term	2798,371	1	2798,371	3527,520	,000	,990
Art * Maus	2,203	3	,734	,926	,438	,072
Art	58,238	1	58,238	73,413	,000	,671
Maus	12,662	3	4,221	5,320	,004	,307
Fehler	28,559	36	,793			
Gesamt	2898,294	44				
Korrigierte Gesamtvariation	102,171	43				

a. Gen Gen = IL-1B

b. R-Quadrat = ,720 (korrigiertes R-Quadrat = ,666)

Tests der Zwischensubjekteffekte[a]

Abhängige Variable: dCT dCT

Quelle	Quadratsumme vom Typ III	df	Mittel der Quadrate	F	Sig.	Partielles Eta-Quadrat
Korrigiertes Modell	149,249[b]	7	21,321	21,138	,000	,800
Konstanter Term	408,135	1	408,135	404,630	,000	,916
Art * Maus	12,581	3	4,194	4,158	,012	,252
Art	121,430	1	121,430	120,387	,000	,765
Maus	12,592	3	4,197	4,161	,012	,252
Fehler	37,321	37	1,009			
Gesamt	571,125	45				
Korrigierte Gesamtvariation	186,569	44				

a. Gen Gen = Col1A1

b. R-Quadrat = ,800 (korrigiertes R-Quadrat = ,762)

Leven-Test Fig. 2 F	**df1**	**df2**	**Sig.**
ADAM10	1,291	7	36	0,283
Col1A1	3,18	7	37	0,010
Collagen 3A1	1,025	7	36	0,431
IL-1B	0,493	7	36	0,833
MMP9	2,864	7	36	0,018
Gpr18 (M1)	1,065	7	38	0,405

Figure 5:

Test bei unabhängigen Stichproben[a]

		Levene-Test der Varianzgleichheit		T-Test für die Mittelwertgleichheit						
									95% Konfidenzintervall der Differenz	
		F	Signifikanz	T	df	Sig. (2-seitig)	Mittlere Differenz	Standardfehler der Differenz	Untere	Obere
dCT dCT	Varianzen sind gleich	1,133	,347	5,800	4	,004	1,844257	,317953	,961479	2,727034
	Varianzen sind nicht gleich			5,800	3,286	,008	1,844257	,317953	,880489	2,808024

a. Gen Gen = Collagen 1A1

Test bei unabhängigen Stichproben[a]

		Levene-Test der Varianzgleichheit		T-Test für die Mittelwertgleichheit						
									95% Konfidenzintervall der Differenz	
		F	Signifikanz	T	df	Sig. (2-seitig)	Mittlere Differenz	Standardfehler der Differenz	Untere	Obere
dCT dCT	Varianzen sind gleich	4,685	,096	6,505	4	,003	1,663250	,255684	,953358	2,373141
	Varianzen sind nicht gleich			6,505	2,556	,012	1,663250	,255684	,763519	2,562980

a. Gen Gen = ADAM10

Test bei unabhängigen Stichproben[a]

		Levene-Test der Varianzgleichheit		T-Test für die Mittelwertgleichheit						
									95% Konfidenzintervall der Differenz	
		F	Signifikanz	T	df	Sig. (2-seitig)	Mittlere Differenz	Standardfehler der Differenz	Untere	Obere
dCT dCT	Varianzen sind gleich	1,426	,298	20,397	4	,000	8,607935	,422016	7,436230	9,779640
	Varianzen sind nicht gleich			20,397	3,349	,000	8,607935	,422016	7,340749	9,875121

a. Gen Gen = MMP9

Test bei unabhängigen Stichproben[a]

		Levene-Test der Varianzgleichheit		T-Test für die Mittelwertgleichheit						
									95% Konfidenzintervall der Differenz	
		F	Signifikanz	T	df	Sig. (2-seitig)	Mittlere Differenz	Standardfehler der Differenz	Untere	Obere
dCT dCT	Varianzen sind gleich	12,449	,024	3,913	4	,017	1,742756	,445366	,506222	2,979290
	Varianzen sind nicht gleich			3,913	2,051	,057	1,742756	,445366	-,128625	3,614136

a. Gen Gen = IL-6

Test bei unabhängigen Stichproben[a]

		Levene-Test der Varianzgleichheit		T-Test für die Mittelwertgleichheit						
									95% Konfidenzintervall der Differenz	
		F	Signifikanz	T	df	Sig. (2-seitig)	Mittlere Differenz	Standardfehler der Differenz	Untere	Obere
dCT dCT	Varianzen sind gleich	,006	,940	-,801	4	,468	-,185172	,231235	-,827183	,456838
	Varianzen sind nicht gleich			-,801	3,998	,468	-,185172	,231235	-,827285	,456941

a. Gen Gen = Collagen 3A1

Test bei unabhängigen Stichproben[a]

		Levene-Test der Varianzgleichheit		T-Test für die Mittelwertgleichheit						
									95% Konfidenzintervall der Differenz	
		F	Signifikanz	T	df	Sig. (2-seitig)	Mittlere Differenz	Standardfehler der Differenz	Untere	Obere
dCT dCT	Varianzen sind gleich	8,606	,043	1,997	4	,117	1,250425	,626268	-,488374	2,989225
	Varianzen sind nicht gleich			1,997	2,095	,178	1,250425	,626268	-1,330040	3,830891

a. Gen Gen = IL-10

Test der Homogenität der Varianzen[a]

dCT dCT

Levene-Statistik	df1	df2	Signifikanz
2,848	5	12	,064

a. Typ Typ = 1 Veh

Figure 6:

Einfaktorielle ANOVA[a]

dCT dCT

	Quadratsumme	df	Mittel der Quadrate	F	Signifikanz
Zwischen den Gruppen	29,930	2	14,965	157,053	,000
Innerhalb der Gruppen	,572	6	,095		
Gesamt	30,501	8			

a. Gen_1 = 1 FGF23

Mehrfachvergleiche[a]

Abhängige Variable: dCT dCT

LSD

(I) Behandlung Behandlung	(J) Behandlung Behandlung	Mittlere Differenz (I-J)	Standardfehler	Signifikanz	95%-Konfidenzintervall	
					Untergrenze	Obergrenze
1 Veh	2 IL-1B	3,979376*	,252038	,000	3,36266	4,59609
	3 IL-1B + rFGF23	3,747012*	,252038	,000	3,13030	4,36373
2 IL-1B	1 Veh	-3,979376*	,252038	,000	-4,59609	-3,36266
	3 IL-1B + rFGF23	-,232364	,252038	,392	-,84908	,38435
3 IL-1B + rFGF23	1 Veh	-3,747012*	,252038	,000	-4,36373	-3,13030
	2 IL-1B	,232364	,252038	,392	-,38435	,84908

*. Die Differenz der Mittelwerte ist auf dem Niveau 0.05 signifikant.

a. Gen_1 = 1 FGF23

Einfaktorielle ANOVA[a]

dCT dCT

	Quadratsumme	df	Mittel der Quadrate	F	Signifikanz
Zwischen den Gruppen	17,794	2	8,897	29,541	,001
Innerhalb der Gruppen	1,807	6	,301		
Gesamt	19,601	8			

a. Gen_1 = 2 Klotho

Mehrfachvergleiche[a]

Abhängige Variable: dCT dCT

LSD

(I) Behandlung Behandlung	(J) Behandlung Behandlung	Mittlere Differenz (I-J)	Standardfehler	Signifikanz	95%-Konfidenzintervall	
					Untergrenze	Obergrenze
1 Veh	2 IL-1B	2,598757*	,448086	,001	1,50233	3,69519
	3 IL-1B + rFGF23	3,256849*	,448086	,000	2,16042	4,35328
2 IL-1B	1 Veh	-2,598757*	,448086	,001	-3,69519	-1,50233
	3 IL-1B + rFGF23	,658091	,448086	,192	-,43834	1,75452
3 IL-1B + rFGF23	1 Veh	-3,256849*	,448086	,000	-4,35328	-2,16042
	2 IL-1B	-,658091	,448086	,192	-1,75452	,43834

*. Die Differenz der Mittelwerte ist auf dem Niveau 0.05 signifikant.

a. Gen_1 = 2 Klotho

Einfaktorielle ANOVA[a]

dCT dCT

	Quadratsumme	df	Mittel der Quadrate	F	Signifikanz
Zwischen den Gruppen	7,328	2	3,664	17,207	,003
Innerhalb der Gruppen	1,278	6	,213		
Gesamt	8,606	8			

a. Gen_1 = 3 AlphaSMA

Mehrfachvergleiche[a]

Abhängige Variable: dCT dCT

LSD

(I) Behandlung Behandlung	(J) Behandlung Behandlung	Mittlere Differenz (I-J)	Standardfehler	Signifikanz	95%-Konfidenzintervall	
					Untergrenze	Obergrenze
1 Veh	2 IL-1B	,374355	,376768	,359	-,54756	1,29627
	3 IL-1B + rFGF23	2,073682*	,376768	,002	1,15176	2,99560
2 IL-1B	1 Veh	-,374355	,376768	,359	-1,29627	,54756
	3 IL-1B + rFGF23	1,699327*	,376768	,004	,77741	2,62124
3 IL-1B + rFGF23	1 Veh	-2,073682*	,376768	,002	-2,99560	-1,15176
	2 IL-1B	-1,699327*	,376768	,004	-2,62124	-,77741

*. Die Differenz der Mittelwerte ist auf dem Niveau 0.05 signifikant.

a. Gen_1 = 3 AlphaSMA

Einfaktorielle ANOVA[a]

dCT dCT

	Quadratsumme	df	Mittel der Quadrate	F	Signifikanz
Zwischen den Gruppen	3,212	2	1,606	16,558	,004
Innerhalb der Gruppen	,582	6	,097		
Gesamt	3,794	8			

a. Gen_1 = 4 Collagen 1A1

Mehrfachvergleiche[a]

Abhängige Variable: dCT dCT

LSD

(I) Behandlung Behandlung	(J) Behandlung Behandlung	Mittlere Differenz (I-J)	Standardfehler	Signifikanz	95%-Konfidenzintervall	
					Untergrenze	Obergrenze
1 Veh	2 IL-1B	,515197	,254273	,089	-,10699	1,13738
	3 IL-1B + rFGF23	1,443684*	,254273	,001	,82150	2,06587
2 IL-1B	1 Veh	-,515197	,254273	,089	-1,13738	,10699
	3 IL-1B + rFGF23	,928487*	,254273	,011	,30630	1,55067
3 IL-1B + rFGF23	1 Veh	-1,443684*	,254273	,001	-2,06587	-,82150
	2 IL-1B	-,928487*	,254273	,011	-1,55067	-,30630

*. Die Differenz der Mittelwerte ist auf dem Niveau 0.05 signifikant.

a. Gen_1 = 4 Collagen 1A1

Einfaktorielle ANOVA[a]

dCT dCT

	Quadratsumme	df	Mittel der Quadrate	F	Signifikanz
Zwischen den Gruppen	161,580	2	80,790	12,858	,007
Innerhalb der Gruppen	37,701	6	6,283		
Gesamt	199,281	8			

a. Gen_1 = 5 MMP9

Mehrfachvergleiche[a]

Abhängige Variable: dCT dCT

LSD

(I) Behandlung Behandlung	(J) Behandlung Behandlung	Mittlere Differenz (I-J)	Standardfehler	Signifikanz	95%-Konfidenzintervall	
					Untergrenze	Obergrenze
1 Veh	2 IL-1B	2,508023	2,046696	,266	-2,50006	7,51611
	3 IL-1B + rFGF23	9,975959*	2,046696	,003	4,96787	14,98404
2 IL-1B	1 Veh	-2,508023	2,046696	,266	-7,51611	2,50006
	3 IL-1B + rFGF23	7,467936*	2,046696	,011	2,45985	12,47602
3 IL-1B + rFGF23	1 Veh	-9,975959*	2,046696	,003	-14,98404	-4,96787
	2 IL-1B	-7,467936*	2,046696	,011	-12,47602	-2,45985

*. Die Differenz der Mittelwerte ist auf dem Niveau 0.05 signifikant.

a. Gen_1 = 5 MMP9

Einfaktorielle ANOVA[a]

dCT dCT

	Quadratsumme	df	Mittel der Quadrate	F	Signifikanz
Zwischen den Gruppen	15,136	2	7,568	7,968	,020
Innerhalb der Gruppen	5,699	6	,950		
Gesamt	20,835	8			

a. Gen_1 = 6 ADAM10

Mehrfachvergleiche[a]

Abhängige Variable: dCT dCT

LSD

(I) Behandlung Behandlung	(J) Behandlung Behandlung	Mittlere Differenz (I-J)	Standardfehler	Signifikanz	95%-Konfidenzintervall	
					Untergrenze	Obergrenze
1 Veh	2 IL-1B	,126051	,795754	,879	-1,82109	2,07319
	3 IL-1B + rFGF23	2,811854*	,795754	,012	,86471	4,75900
2 IL-1B	1 Veh	-,126051	,795754	,879	-2,07319	1,82109
	3 IL-1B + rFGF23	2,685803*	,795754	,015	,73866	4,63294
3 IL-1B + rFGF23	1 Veh	-2,811854*	,795754	,012	-4,75900	-,86471
	2 IL-1B	-2,685803*	,795754	,015	-4,63294	-,73866

*. Die Differenz der Mittelwerte ist auf dem Niveau 0.05 signifikant.

a. Gen_1 = 6 ADAM10

Einfaktorielle ANOVA[a]

dCT dCT

	Quadratsumme	df	Mittel der Quadrate	F	Signifikanz
Zwischen den Gruppen	6,589	2	3,295	47,211	,000
Innerhalb der Gruppen	,419	6	,070		
Gesamt	7,008	8			

a. Gen_1 = 7 Collagen 3A1

Mehrfachvergleiche[a]

Abhängige Variable: dCT dCT

LSD

(I) Behandlung Behandlung	(J) Behandlung Behandlung	Mittlere Differenz (I-J)	Standardfehler	Signifikanz	95%-Konfidenzintervall	
					Untergrenze	Obergrenze
1 Veh	2 IL-1B	2,090115*	,215696	,000	1,56233	2,61790
	3 IL-1B + rFGF23	,909830*	,215696	,006	,38204	1,43762
2 IL-1B	1 Veh	-2,090115*	,215696	,000	-2,61790	-1,56233
	3 IL-1B + rFGF23	-1,180285*	,215696	,002	-1,70807	-,65250
3 IL-1B + rFGF23	1 Veh	-,909830*	,215696	,006	-1,43762	-,38204
	2 IL-1B	1,180285*	,215696	,002	,65250	1,70807

*. Die Differenz der Mittelwerte ist auf dem Niveau 0.05 signifikant.

a. Gen_1 = 7 Collagen 3A1

Leven-Test Fig. 2 F		df1	df2	Sig.
FGF23	0,31	2	6	0,744
Klotho	1,101	2	6	0,392
AlphaSMA	4,975	2	6	0,053
Collagen 1A1	2,639	2	6	0,151
MMP9	11,19	2	6	0,059
ADAM10	1,619	2	6	0,274
Collagen 3A1	0,539	2	6	0,609